MASTERARBEIT

Titel der Masterarbeit

,,Interferon Immune Response to *Candida glabrata* in Dendritic Cells*''*

verfasst von

Valentina Stolz BSc

Angestrebter akademischer Grad

Master of Science (MSc)

Wien, 2014

Table of Contents

1 Abstract

Candida glabrata is one of the most prevalent fungal pathogens in human. In the healthy host, *C. glabrata* does not lead to an infection. However, in immunocompromised individuals, *C. glabrata* can cause mucosal and blood stream infections. Candida infections became a major health problem due to the high incidence of immunosuppression, with *C. glabrata* accounting for ~20% of all Candida blood stream infections worldwide. As antigen - presenting phagocytes, dendritic cells play a crucial role in the detection and removal of *C. glabrata*. Previous reports suggest type I IFNs as being one of the most important signaling molecules during infections with Candida species. In this study, murine bone - marrow - derived dendritic cells (BMDCs) were differentiated *in vitro*, and time - dependent transcriptomics of both *M. musculus* and *C. glabrata* RNA changes was performed. To address the role of type I IFNs during *C. glabrata* - induced immune responses, not only wild type, but also *Ifnar1*$^{-/-}$ cells, which lack a functional receptor for type I IFNs, were used for the experiments. Parallel dual - species RNA sequencing (RNA Seq), which represents a high throughput method that allows one to look at the whole transcriptome of one or more organisms at the same time, was performed. After sequencing, the results were analyzed bioinformatically. Dual - species differential gene expression was investigated both in murine and in Candida cells. We deduced a list of gene ontology (GO) terms to indicate the importance of specific groups of genes and to show the high complexity of interacting components during an immune response. Additionally, we identified 3 novel genes in *C. glabrata*, that seem to be important during infection, since the loss of these genes resulted in a reduced survival rate of *C. glabrata* during infection with BMDCs. These genes have, to our knowledge, not been associated with *C. glabrata* infections so far.

2 Introduction

2.1 Candida species

Candida species are unicellular, fungal organisms that can live as opportunistic pathogens in a variety of hosts, most importantly human[1]. Even more important is the fact, that the existence of Candida species is not only limited to an opportunistic way of life, but can also become pathogenic under special circumstances. Although most species that belong to the Candida genus are non - pathogenic, there are species that can lead to severe diseases in human, making them relevant microorganisms in the medical sector[2]. Although much research has been done on Candida in the last couple of decades, underlying mechanisms of virulence in different strains are still not well understood. The most studied organism of the Candida genus is *Candida albicans*, which is also the most prevalent. However, medical incidents caused by other species are constantly increasing[3].

Candida belongs to the family of Saccharomycetaceae (yeasts) that includes a huge variety of different species. The morphology of Candida can be described as whitish - cream colonies when grown on YPD plates. Their appearance observed under the light microscope depends on the morphological state they are currently in. Fungal species in general can grow in one of three different morphologies:

1. Yeast form
2. Pseudohyphae
3. Hyphae

C. albicans, for example, can switch between those three states, in accordance to its environment[4] (Figure 1). However, not every Candida species can grow in all three morphologies, for example *C. glabrata*, which can only switch between

yeast and pseudohyphal growth[5]. Interestingly, the formation of hyphae is a very important virulence trait in *C. albicans*, as it enables the pathogen to escape from immune cells and invade host tissues by penetrating the cell with its hyphae[6]. The formation of hyphae is however not inevitable for virulence in the host, which can be seen by existence of pathogenicity in non - hyphal fungi, like *C. glabrata*.
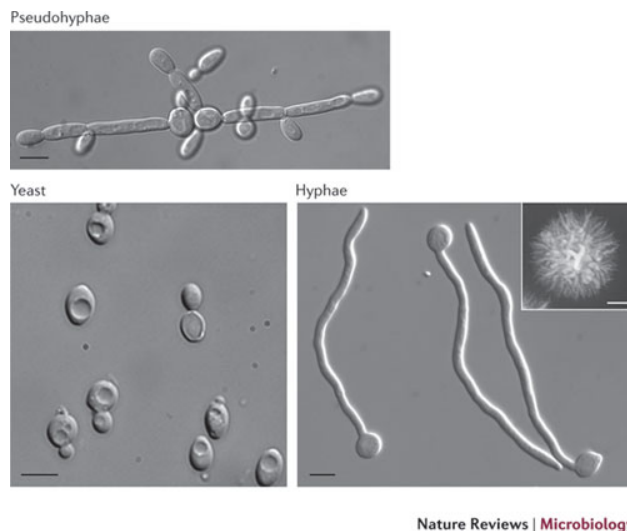
Nature Reviews | Microbiology

Figure 1. Comparison of yeast, pseudohyphal and hyphal growth in *C. albicans*

The figure shows *C. albicans* observed under the light microscope during pseudohyphal growth (top), yeast growth (bottom left) and hyphal growth (bottom right). Taken from Sudberry (2011)[7].

Candida species are widely distributed and can be isolated mainly from the gastrointestinal tract of humans and other mammals, but can also be found in the environment, for example soil[8]. Only few species of Candida have been shown to be virulent and are therefore clinically relevant. For example, *Candida albicans*, *Candida glabrata*, *Candida tropicalis* and *Candida parapsilosis* are the most common among others[9]. The risk of getting infected by Candida species depends on a variety of factors, which includes age, genetic factors and general health status. For example, it has been shown that infants and children are more prone in getting infected with Candida parapsilosis than adolescent people[10,11]. Another risk factor that contributes in candidemia includes hospitalization, especially with patients that are kept in intensive care units and people that have undergone surgeries followed by antibiotic therapy[10,11]. It has been reported that Candida is the fourth most common nosocomial bloodstream pathogen in the US[12]. In general, candidemia is a serious problem in patients suffering from immunosuppressive diseases, like acquired immunodeficiency syndrome

(AIDS)[13]. Non-surprisingly, it has been shown that genetic disorders can contribute to severe infections with Candida species[14], especially the loss of cytokines, transcription factors (TFs) and other signaling molecules, for example toll - like receptor 7 (TLR7)[15], signal transducer and activator of transcription 1 (STAT1)[11], Dectin-1[16], caspase recruitment domain-containing protein 9 (CARD9)[17] and Jagunal homolog 1 (Jagn1)[18]. When studying Candida in the lab, the genetic susceptibility is a factor that has to be considered during experimental design *in vitro* and *in vivo*, since it has been shown that some mouse models are more susceptible to systemic candidemia than others[19].

In a majority of the population, Candida species live as opportunistic organisms on mucosal surfaces like skin[20]. However, under special circumstances, like mentioned above, those Candida species can lead to superficial infections, like oral candidiasis, called thrush[21]. Also the vaginal[22] or esophageal mucous[23] can be affected. Other areas of superficial infections with Candida affect cutaneous areas and the nails[24]. A serious problem is the fact, that Candida can cause systemic infections[2]. During systemic candidiasis, the pathogen spreads through the body via the bloodstream and eventually causes the infection of a whole organ. It can further induce infection of multiple organs, a condition called invasive candidiasis[25]. Organs affected by systemic candidiasis usually include kidneys, liver, brain, spleen and others[26]. Systemic infections by Candida are common in people suffering from a malfunctioning immune response and can be lethal with a mortality rate of up to 40%[25], especially when it leads to the development of sepsis. Sepsis is an inflammation affecting the whole body, leading to organ dysfunction and death[27]. Superficial, as well as systemic candidiasis is usually treated with antifungal medication like fluconazole, imidazole, caspofungin and echinocandins[28,29]. However, due to the high abundance of antifungal resistance in Candida species, treatment of candidiasis, superficial as well as systemic, became more and more problematic[30–32].

2.2 Candida glabrata

C. glabrata is relatively small compared to other Candida yeasts (1 - 4 *µ*m)[33]. In comparison to its more virulent relative *C. albicans*, *C. glabrata* is haploid without the ability to mate in order to form diploids[34]. It grows as blastoconidia (yeast morphology) and is not able to form true hyphae[33,35]. However, it is able to produce pseudohyphae in response to nitrogen source starvation, a trait that is often related to its pathogenicity[5,36]. Despite its name, *C. glabrata* is actually more related to *Saccharomyces cerevisiae* than to other Candida species (Figure 2). The evolutionary divergence between *C. glabrata* and *S. cerevisiae* is considered to be 100 - 300 million years. Whereas, *C. albicans* and *C. glabrata* differ by up to 800 million years[37].
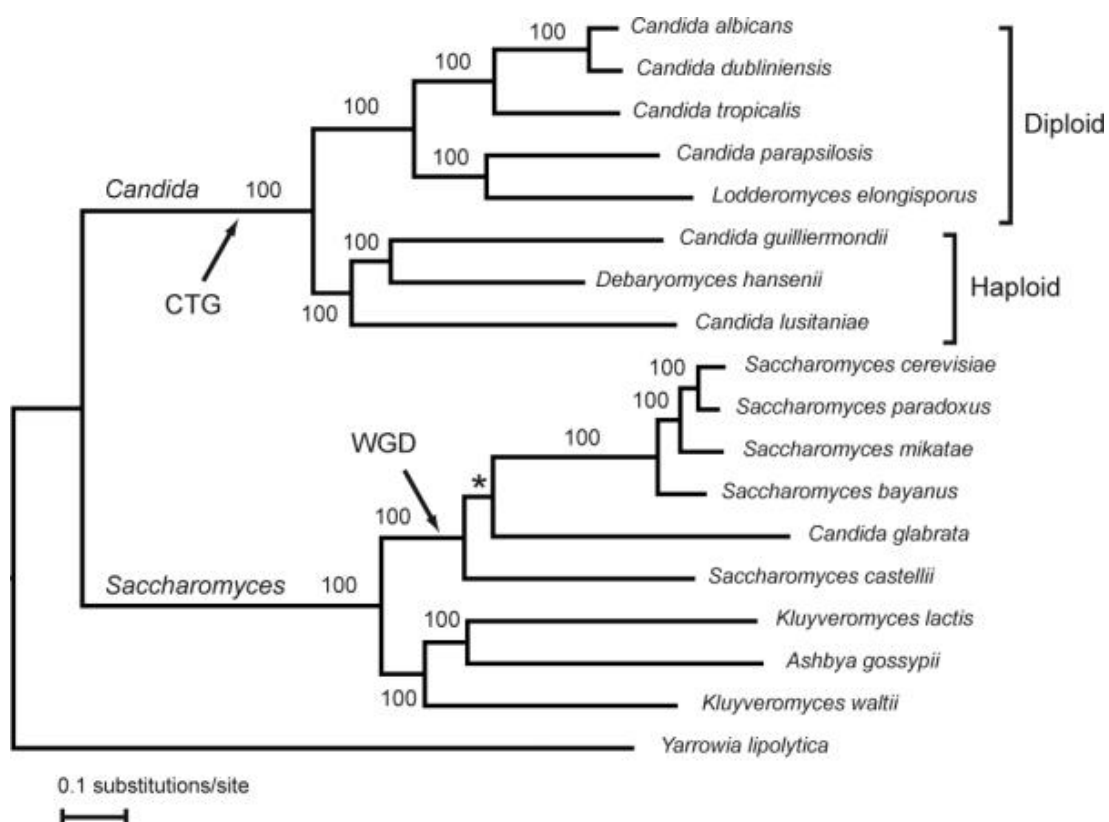
Figure 2. Phylogenetic tree of the Candida and the Saccharomyces clade

This figure shows the phylogeny of the Candida and the Saccharomyces clade. Note that *C. glabrata* belongs to the Saccharomyces clade phylogenetically. Therefore *C. glabrata* is often considered to be more related to non - Candida fungi. Taken from Butler et al. 2009[7].

During its evolution, *C. glabrata* has lost many genes that are present in *S. cerevisiae*, but has also gained unique genes that are important for virulence[38]. Losses include mainly genes that are responsible for metabolic processes, such as the *de novo* synthesis of nicotinic acid, a precursor of nicotinamide adenine dinucleotide (NAD+)[38]. Therefore, *C. glabrata* is dependent on the uptake of nicotinic acid from the host[39]. However, in spite of having lost some metabolic genes, *C. glabrata* has gained functions that made it to a successful human pathogen. For example, *C. glabrata* is able to adhere to mammalian host cells[38]. The genes responsible for this virulence trait are called *EPA* genes, which encode a variety of fungal adhesins. It is assumed that some of those genes are also crucial for the formation of biofilms, since it has been shown that the lack of *EPA6* leads to a reduced formation of biofilms *in vitro*[39]. In addition, *C. glabrata* exhibits a high resistance to environmental stress, especially nutrient starvation and oxidative stress[38]. This enables *C. glabrata* to survive inside the host cells upon phagocytosis[40].

2.3 Pathogenicity of *C. glabrata*

After *C. albicans*, *C. glabrata* is one of the most prevalent fungal pathogens in humans and the second most prevalent pathogen of the Candida species[41]. In the healthy host, *C. glabrata* does not lead to an infection, and although not being as invasive as its relative *C. albicans*, *C. glabrata* can cause severe diseases in immunocompromised individuals[42]. *C. glabrata* can lead to both superficial as well as systemic infections[35]. Due to the high incidence of immunosuppression nowadays, Candida infections became a major health problem, with *C. glabrata* accounting for up to 20% of all Candida blood stream infections worldwide[39]. Infections by *C. glabrata* are mostly mucosal or systemic, often derive from nosocomial sources like hospital personnel[33] and have mortality rates similar to that of *C. albicans*[40,43]. One of *C. glabratas* major virulence factors is its high intrinsically resistance to various antifungal drugs. These drugs include azoles, echinocandins and polyenes, all of them interacting with the cell wall of

Candida[29]. One mechanism responsible for the acquisition of drug resistance is the expression of ABC transporters that work as drug efflux pumps leading to multidrug resistance[30–32]. In addition, recent findings suggest chromatin modifications as a possibility of how *C. glabrata* is able to avoid being killed[39].

It has been shown that antifungal resistance of *C. glabrata* underlies geographical variances[10]. As mentioned above, *C. glabrata* can adhere to host cells and is also able to form biofilms, not only on host tissue, but also on medical devices, such as catheters[44]. Candida biofilms usually consist of a bilayer of matrix - enclosed yeast cells, that show high resistance to various drugs. It has also been shown that Candida biofilms can be composed of a mixture of multiple species of Candida and bacteria[45].

When studying virulence of *C. glabrata in vivo* in mouse models, the low pathogenicity of this fungus becomes apparent. Infection of mice with *C. glabrata* leads to systemic candidiasis. However, it does not lead to mortality in infected mice. Only the tail vein infection with high fungal burdens and the administration of immunosuppressive drugs results in death. Another possibility to study the virulence of low - pathogenic fungi like *C. glabrata* is the investigation of tissue colonization after infection[46]. However, the outcome of infection depends on the mouse and *C. glabrata* strains used[42]. Evidence suggests that the survival mechanisms of *C. glabrata* inside the host are very different from other Candida species, like *C. albicans*. It is so far unknown how *C. glabrata* is able to invade the host tissue without the ability to form hyphae and while causing little or no cell damage. Some reports suggested the formation of pseudohyphae as a possible mechanism to invade host tissue[5,36]. However, the low production of inflammatory cytokines after infection indicates invasion of *C. glabrata* into the host without causing tissue damage[36,42]. Possible mechanisms for colonization could be endocytosis[47] or autophagy[48] of the fungus by host cells.

2.4 Dendritic cells as first line of defense against invading pathogens

The immune system is essential for survival and consists of a variety of protecting mechanisms. The first barrier that guards against pathogens is the skin. However, when the skin is injured, pathogens can invade the tissue causing infection. Therefore, the immune system consists of plenty of cell types, that carry out many different functions in the body. Some cells are responsible for phagocytosis of pathogens followed by antigen presentation. Others, in contrast, remove pathogens by inducing programmed cells death in infected cells. And yet others are specialized in the production of antibodies, which leads to humoral immunity. Apart from antibodies, humoral immunity comprises many other proteins that have protecting and opsonizing properties.

However, the immune system is not only responsible for fighting pathogens, but also immune surveillance. It copes with the difficult task of keeping the immune response in balance. The mammalian immune system is generally divided into two subunits, the innate immune system and the adaptive immune system. The innate immune system displays limited diversity against pathogens, but is quick in recognizing and destroying them. The adaptive immune system in contrast can adapt to an enormous amount of antigens and possesses the ability to maintain memory once an antigen has been recognized and neutralized. It takes, however, several days to weeks to develop. Therefore, interplay between these two systems is crucial[49]. One cell type that enables this interplay are dendritic cells (DCs). DCs, together with neutrophils and macrophages, form the first lines of defense against invading pathogens. Yet, dendritic cells have a fundamental role in building a bridge between the innate and the adaptive immune system[50]. One of their objectives is to work as phagocytic cells, presenting surface bound antigen to naïve T cells[51]. In order to do so, dendritic cells process invading microbes and further present antigens on their surfaces using specialized proteins called MHC molecules (major histocompatibility complex)[52]. In human, the genes encoding MHC molecules are called human leukocyte antigen (HLA)[49]. Two classes of MHC molecules are known: MHC class I is responsible for the

presentation of antigen that was processed intracellularly, for example viruses that infect the cell. Antigen that is presented on MHC class I molecules is recognized by CD8^{+} T cells and leads to the formation of cytotoxic T cells. In contrast, MHC class II molecules present antigen that is processed extracellularly in vesicles, gets recognized by CD4^{+} T cells and leads to the formation of helper T cells. Their efficiency in presenting antigen to T cells is facilitated by the expression of costimulatory molecules on the surface of DCs[51,53]. In addition to priming the immune response to foreign antigens, DCs are also responsible in inducing self - tolerance[54].

A huge variety of different DC subsets is known and they are resident to many tissues. For example in the skin, where they are commonly referred to as Langerhans cells[55]. The multitude of different subsets complicates studies with DCs. Research is even more hindered due to their close similarity to other cell types like macrophages[56]. Much debate is ongoing about the categorization of DCs. One of the general opinion however states that DCs descend either from a plasmacytoid or from a myeloid lineage[56,57]. During our experiments, we used murine bone marrow - derived myeloid dendritic cells (mDCs), also called conventional dendritic cells. mDCs derive from monocytes and therefore share common features with macrophages[58].

2.4.1 Interaction of *C. glabrata* with phagocytic cells

As mentioned above, *C. albicans* can evade phagocytic killing by producing long hyphae, which are able to pierce the cell membrane[6]. Once outside of the cell, *C. albicans* can replicate and spread through the body via the bloodstream. It can then lead to superficial and systemic infections[6]. *C. glabrata* however, has evolved very different strategies to survive inside the host. It has been shown that *C. glabrata* can survive inside mice for several weeks, while only causing a marginal immune response which is characterized by the low production of inflammatory cytokines[36,42]. DCs, but also macrophages and neutrophils are responsible in detecting and engulfing foreign invaders, which leads to the formation of a phagosome. The phagosome then matures and fuses with

lysosomes, to form a so - called phagolysosome[61]. The lysosome is acidic and contains degradative enzymes, reactive oxygen species (ROS) and reactive nitrogen species (RNS) that are intended to kill the pathogen. In addition, nutrients and certain trace elements are abundant[49,61,62]. *C. glabrata*, however, has evolved a way to survive this stress. Although the mechanisms by which this fungus is able to do so are not yet completely understood, it is known that *C. glabrata* is able to survive inside the phagolysosome, and even replicates within it. It does so by altering the phagosomal maturation and actively preventing its acidification[40,63,64]. In addition, *C. glabrata* is highly resistant to oxidative stress[63,64], and has developed mechanisms to acquire nutrients and trace elements, especially iron, in the phagosome[64]. During survival and replication, *C. glabrata* causes relatively low damage to the host cell. It does not induce apoptosis in the phagocyte, but eventually leads to rupture of the cell after excessive replication[63,64]. It is not known whether *C. glabrata* actively lyses the cell in order to escape, or whether cell lysis results from mechanical forces due to shortage of space caused by replicating fungi[63]. The ability of surviving inside phagocytic cells is not limited to *C. glabrata* and has also been shown for other Candida spp[65].

2.5 The role of interferons during infections

Interferons (IFNs) are cytokines important during immune response against invading pathogens[66], like viruses, bacteria[67] and fungi[68]. Cells that have encountered a pathogen release interferons in order to recruit immune cells and to signal to nearby cells[69]. Three types of interferons are known (type I - type III). Type III interferons (type III IFNs) are geographically restricted, and are most likely important in resistance to viral infections[70]. Type I interferons (type I IFNs) are secreted by many cell types and are responsible in recruiting inflammatory phagocytes[71]. Several type I IFNs are known, with the main subsets being IFN-α and IFN-β. When the cell is challenged by a pathogen, IFN-β is expressed, released to the extracellular space and is then able to bind to the type I IFN receptor (IFNAR) in an autocrine or paracrine fashion. The IFNAR is a

heterodimer composed of two subunits, IFNAR1 and IFNAR2. Binding of IFN-β to the IFNAR leads to the expression of IFN-α, which is also secreted and also works as ligand for the IFNAR. This mechanism gives rise to an inflammatory amplification loop by constantly expressing type I IFNs. Many transcription factors (TFs) and proinflammatory cytokines are involved in this process, such as interferon regulatory factor 3 (IRF3), IRF7 and STATS (Figure 3). In uninfected cells, binding of type I IFNs leads to the formation of an antiviral state, meaning that those cells become more resistant to infections. In infected cells, type I IFNs enhance the susceptibility to killing by cytotoxic T cells[49,69,72–74].
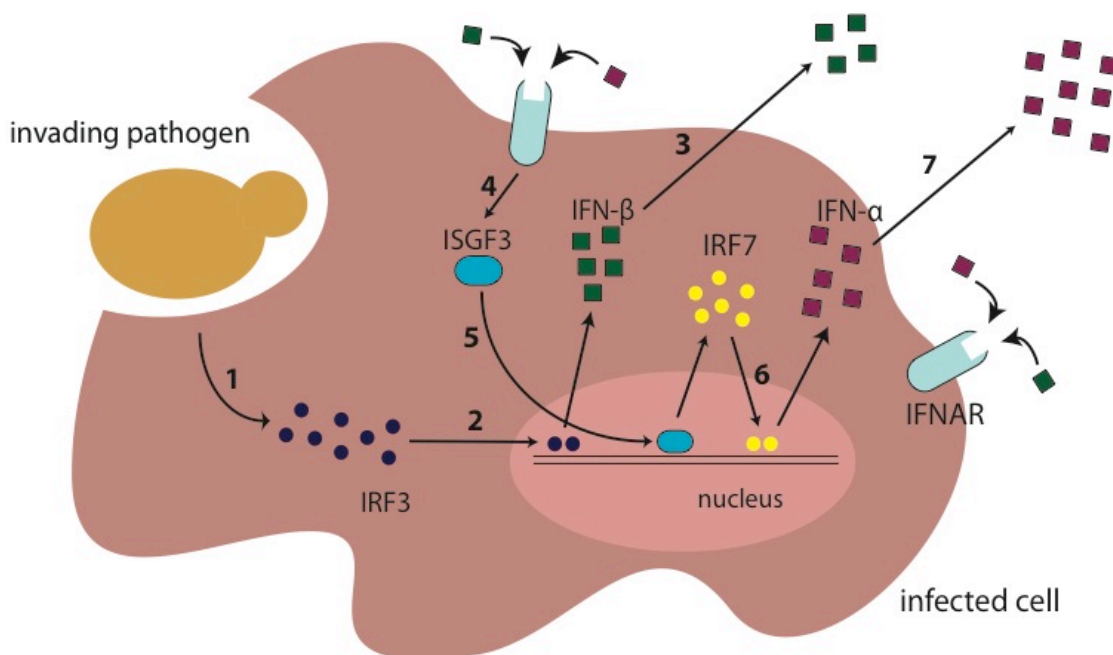
Figure 3. Type I IFNs release after infection leads to the formation of an inflammatory loop

1. Detection of pathogens via membrane bound or cytoplasmic pattern recognition receptors leads to the phosphorylation of interferon regulatory factor 3 (IRF3). 2. IRF3 further migrates into the nucleus where it acts as a TF for IFN-β together with activator protein 1 (AP-1) and the NFκB subunits p50 and p65. 3. IFN-β is then transported outside of the cell where it binds to the IFNAR either in a paracrine or autocrine fashion. 4. Binding of IFN-β leads to the formation and phosphorylation of STAT1/STAT2 heterodimers, which further fuse with IRF9 to form a complex called interferon - stimulated gamma factor 3 (ISGF3). 5. ISGF3 is then transported into the nucleus and acts as a TF for numerous pro - inflammatory proteins, one of them being IRF7. Once the cell has reached this point, it is in a condition called antiviral state. 6. IRF7 again can be phosphorylated and act as a TF for IFN-α. 7. IFN-α can then be transported out of the cell, bind to the IFNAR and therefore create an inflammatory loop.

Type II interferons (type II IFNs) consist only of one member, namely IFN-γ. IFN-γ is expressed by T cells and natural killer cells[49,69]. Its main purpose is to recruit

leucocytes to the site of infection, to activate macrophages, to trigger the maturation of Th1 effector cells from naïve CD4^{+} T cells and to promote isotype switching in B cells[75]. It therefore has an important role in triggering the immune response and further enhancing inflammation.

2.5.1 Type I interferons during infection with Candida

It has been shown that once phagocytosed, *C. glabrata* leads to high expression of IFN-β in mDCs *in vitro*. Interestingly, type I interferons favor the persistence of *C. glabrata* in host tissues[15]. We think that the expression of type I interferons is detrimental to the host during Candida infections, since it has been shown that mice lacking a functional subunit of the IFNAR (*Ifnar1^{-/-}*) are more likely to successfully survive infections with *C. albicans*[71]. *Ifnar1^{-/-}* cells are able to produce and excrete IFN-β. However, they cannot induce an antiviral state due to the fact, that the IFNAR cannot bind its ligand. These observations suggest that the pathogenicity during Candida infections is not caused by the fungus itself, but by tissue damage due to a hyperreactive immune response[71]. Other papers suggest type I interferons as crucial signaling molecules in the clearance of Candida infections[76]. These contradictive findings however could be explained by the use of different mouse and Candida strains.

2.6 Dual species RNA sequencing approach

RNA sequencing (RNA Seq) is a genome - wide sequencing method. It is the most effective method when investigating quantitative transcriptomics[77]. In contrast to DNA sequencing, it provides information on RNA sequences and their abundance[78] (Figure 4). Most researchers are interested in differential gene expression while comparing two different conditions. Therefore, messenger RNA (mRNA) sequences, which are the direct read - out for gene expression, are the object of interest. Great amounts of ribosomal RNA (rRNA) can be found in a cell. Those have to be depleted in order to gain a high coverage for mRNA[79]. RNA

Seq shows low background noise and is highly quantitative as long as coverage is sufficient[80]. Therefore precise results can be given about gene expression levels during the experimental conditions. In contrast to RNA microarrays, the genome sequence does not have to be known. This allows *de novo* sequencing from organisms whose genome sequence is yet unknown[81]. Cost reductions in library preparation and sequencing itself are responsible for the increase in studies that use RNA Seq[80].
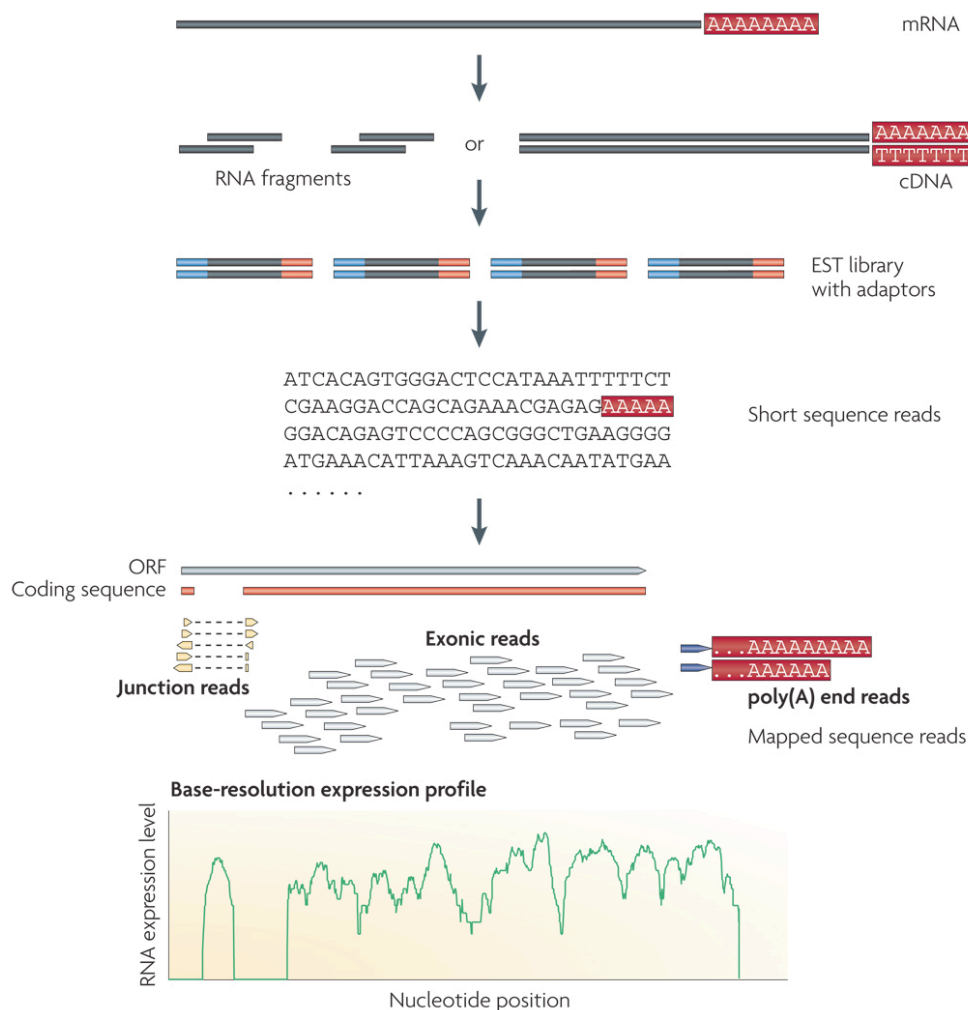
Figure 4. Scheme showing the typical workflow of an RNA sequencing experiment.

In most cases, mRNA is obtained, either by rRNA depletion of poly(A) RNA enrichment. The RNA is further fragmented and transcribed into cDNA (or *vice versa*). Several steps of purification and library preparation are necessary to obtain short cDNA sequences, including the ligation of adapters to the sequences. Due to fact that only sequences derived from mRNA are being sequenced, exonic reads will be obtained, giving you an exact prediction of the genes being expressed. Taken from Wang et al. (2009)[80].

Since our lab is working on the interactions between host immune cells and Candida, we are mainly interested in methods, that enable us to observe the activities of both organisms while interacting with each other. Many studies have shown the success of simultaneous, dual - species RNA Seq, which allows one to gain information about two organisms at the same time[82–86]. Our lab has recently created an interspecies regulatory network between BMDCs and *C. albicans* using time - resolved, simultaneous, dual - species RNA Seq[86]. Due to the huge amount of information that is produced using this kind of system biology approaches, one of the most important steps during experimental design are the right choice of bioinformatical analysis and the subsequent validation[87,88].

2.7 Aims of this study

- We wanted to decipher the time - dependent changes in gene expression in dendritic cells and *C. glabrata* caused during infection.
- In order to do so, we chose a high - throughput approach, namely dual - species RNA sequencing
- This allowed us to investigate the transcriptomes of both organisms at the same time.
- One of the major goals was to identify genes that are differentially expressed during infection.
- Additionally, we were interested to which extent type I IFNs contribute to the immune response to *C. glabrata*, since it is known that those cytokines have a major influence in the outcome of fungal infections.
- To address this, we chose to work with dendritic cells impaired in type I interferon signaling.

3 Results

3.1 Growth curve of *C. glabrata*

Since we used DMEM, which was supplemented with 10% FCS, Penicillin and Streptomycin, for all of our interaction studies, we were interested whether growth of *C. glabrata* would be altered in supplemented DMEM compared to liquid YPD when incubated in Erlenmeyer flasks at 30°C and 220 rpm. Therefore, we created a growth curve using 3 replicates by measuring the absorbance at 600nm. Interestingly, there were striking differences in growth (Figure 5). Almost no growth of *C. glabrata* could be detected in supplemented DMEM. However, previous results suggested, that *C. glabrata* grew in supplemented DMEM during interaction studies with BMDCs, which was visible with the naked eye. Therefore, we assumed that growth of *C. glabrata* in supplemented DMEM during interaction studies was enabled either by the higher temperature (37°C), by the presence of host cells, or by the possibility of *C. glabrata* to adhere to the surface of cell culture - treated dishes. To answer this question, another growth curve was generated by using cell culture - treated dishes instead of Erlenmeyer flasks, and incubation at 37°C in 5% CO_2 atmosphere without rotation. As can be seen in Figure 6, growth of *C. glabrata* in supplemented DMEM was partially restored under those conditions. However, growth of the fungus was still impaired in supplemented DMEM compared to YPD. A third growth curve was generated in order to see whether the increased temperature or the possibility to adhere was responsible for growth of *C. glabrata* in DMEM. Growth curves were generated using cell culture - treated dishes and incubation at 30°C without rotation (Figure 7). Apparently, growth of *C. glabrata* in supplemented DMEM is dependent on higher temperature (37°C), since the growth in culture - treated dishes at 30°C leads to a lack of growth in DMEM. We therefore assume that nutrients and other components in the DMEM are not sufficient for growth of *C. glabrata* at 30°C. In contrast, it seems that DMEM blocks growth of *C. glabrata* at low temperatures, a phenomenon that can partially be overcome when incubating the plates at 37°C.
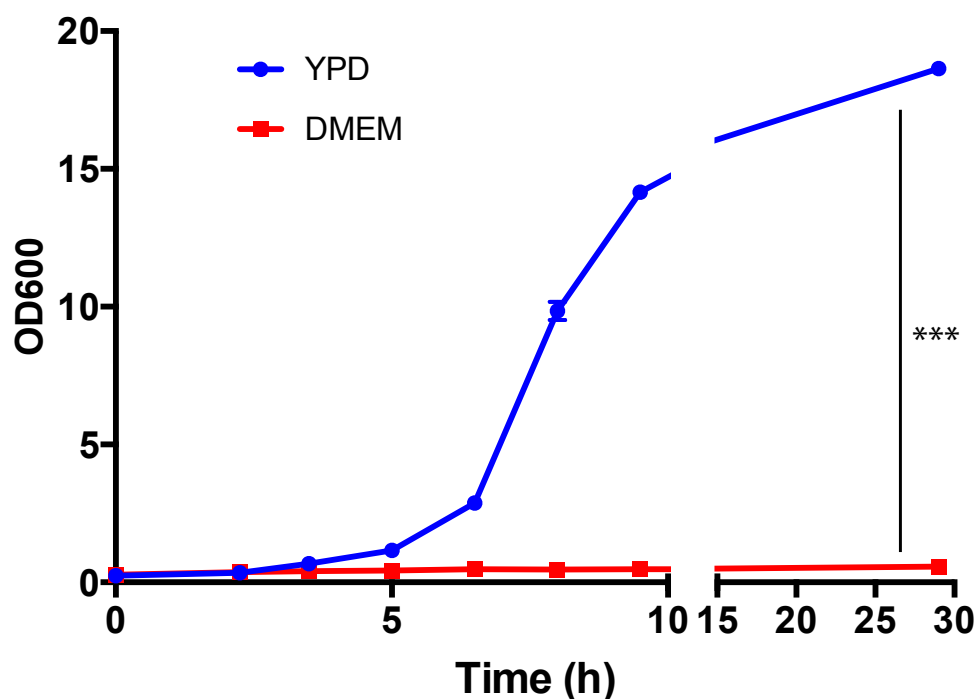
Figure 5. Growth curve of *C. glabrata* in YPD and supplemented DMEM

Growth curve analysis was carried out using either YPD or DMEM, which was supplemented with 10% FCS, Penicillin and Streptomycin, in Erlenmeyer flasks. The samples were incubated at 30°C and 220 rpm. Growth was determined over a time course of 30 hours. Statistical analysis was carried out using an unpaired student's t - test. P - value > 0.001 is indicated by ***.
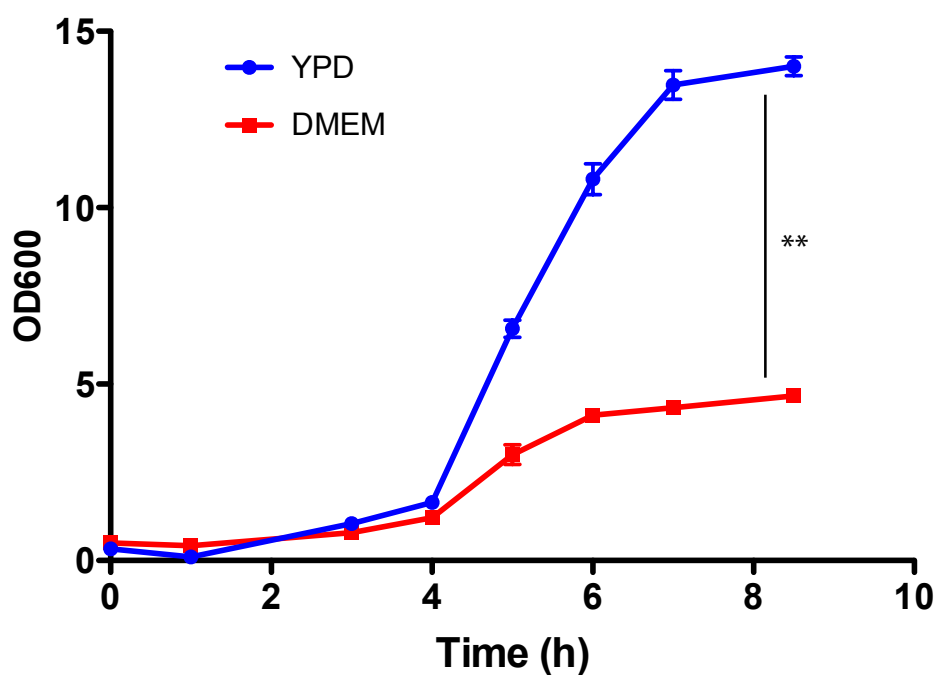
Figure 6. Growth curve of *C. glabrata* in YPD and supplemented DMEM in cell culture - treated dishes at 37°C

Growth curve analysis was carried out using either YPD or DMEM, which was supplemented with 10% FCS, Penicillin and Streptomycin, in cell culture - treated dishes. The samples were incubated at 37°C without rotation. Growth was determined over a time course of 9 hours. Statistical analysis was carried out using an unpaired student's t - test. P - value > 0.01 is indicated by **.
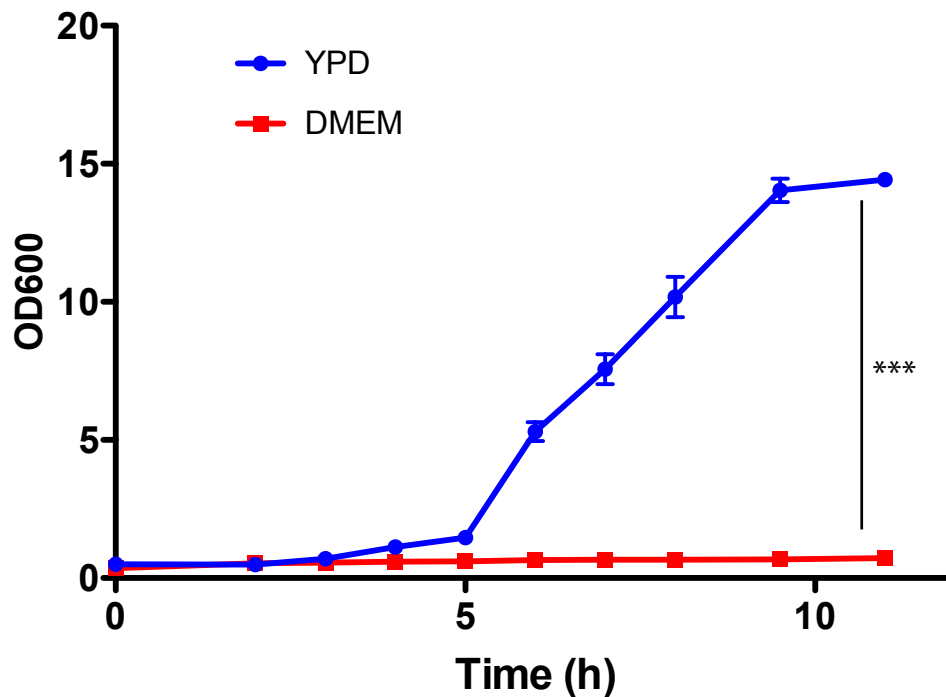
Figure 7. Growth curve of *C. glabrata* in YPD and supplemented DMEM in cell culture - treated dishes at 30°C

Growth curve analysis was carried out using either YPD or DMEM, which was supplemented with 10% FCS, Penicillin and Streptomycin, in cell culture - treated dishes. The samples were incubated at 30°C without rotation. Growth was determined over a time course of 11 hours. Statistical analysis was carries out using an unpaired student's t - test. P - value > 0.001 is indicated by ***.

3.2 Phagocytosis assay

We wanted to exclude the possibility that altered gene expression in the *Ifnar*-/- mutant is caused by a lack in phagocytic uptake of *C. glabrata* by BMDCs, and not by the mutation itself. Therefore a phagocytosis assay was performed with WT and *Ifnar*-/- BMDCs. Since we assumed that the uptake of Candida by DCs happens quite quickly, we chose the following time points of infection for our assay: 15 min, 30 min, 45 min and 90 min. This assay works by infecting phagocytic cells with fluorescently stained Candida, followed by the

measurement of fluorescence per cell. The more Candida the cell has taken up, the stronger the fluorescent signal will be. To begin with, we wanted to make sure, that our Candida culture was stained correctly with Alexa fluor 488. Therefore, we performed FACS analysis of unstained Candida versus stained Candida (Figure 8). After confirming the successful use of Alexa Fluor 488, we compared the fluorescence of uninfected BMDCs with BMDCs infected for 30 minutes (Figure 9). This was done both for WT and *Ifnar*^{-/-} cells. We can see, that infected cells are displayed by a stronger fluorescence, indicating the uptake of fluorescently stained Candida. Additionally, we compared the uptake of *C. glabrata* by WT and *Ifnar*^{-/-} BMDCs 30 and 90 minutes after infection. In Figure 10 we cannot see a clear difference between WT and *Ifnar*^{-/-} BMDCs. However, there is a significant difference in the uptake of *C. glabrata* 30 minutes after infection (Figure 11). Yet, there is no significant difference in the uptake of *C. glabrata* after 45 or 90 minutes and since the earliest time point in our sequencing experiment is 60 minutes, we were not concerned that this result would influence our data.
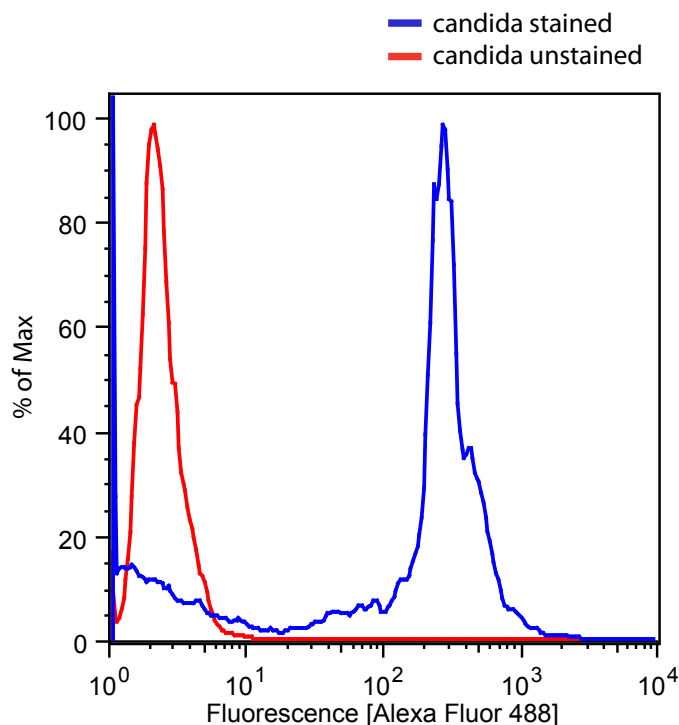
Figure 8. FACS analysis of unstained vs. stained Candida using Alexa Fluor 488

Fluorescence of *C. glabrata* cells was determined using FACS analysis with stained (blue) and unstained (red) *C. glabrata*. Cells were stained using Alexa Fluor 488.
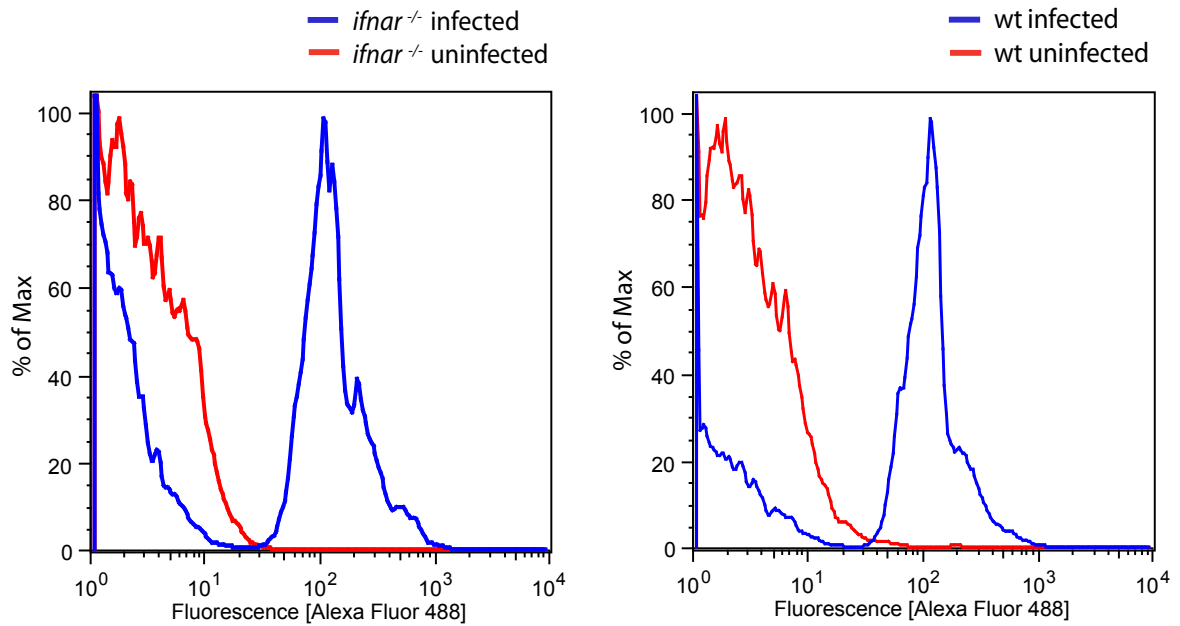
Figure 9. FACS analysis of infected vs. uninfected BMDCs using Alexa Fluor 488

Phagocytic uptake was determined using FACS analysis with either infected (blue) or uninfected (red) BMDCs. Uptake of fluorescently stained *C. glabrata* is displayed as an increase of fluorescence.
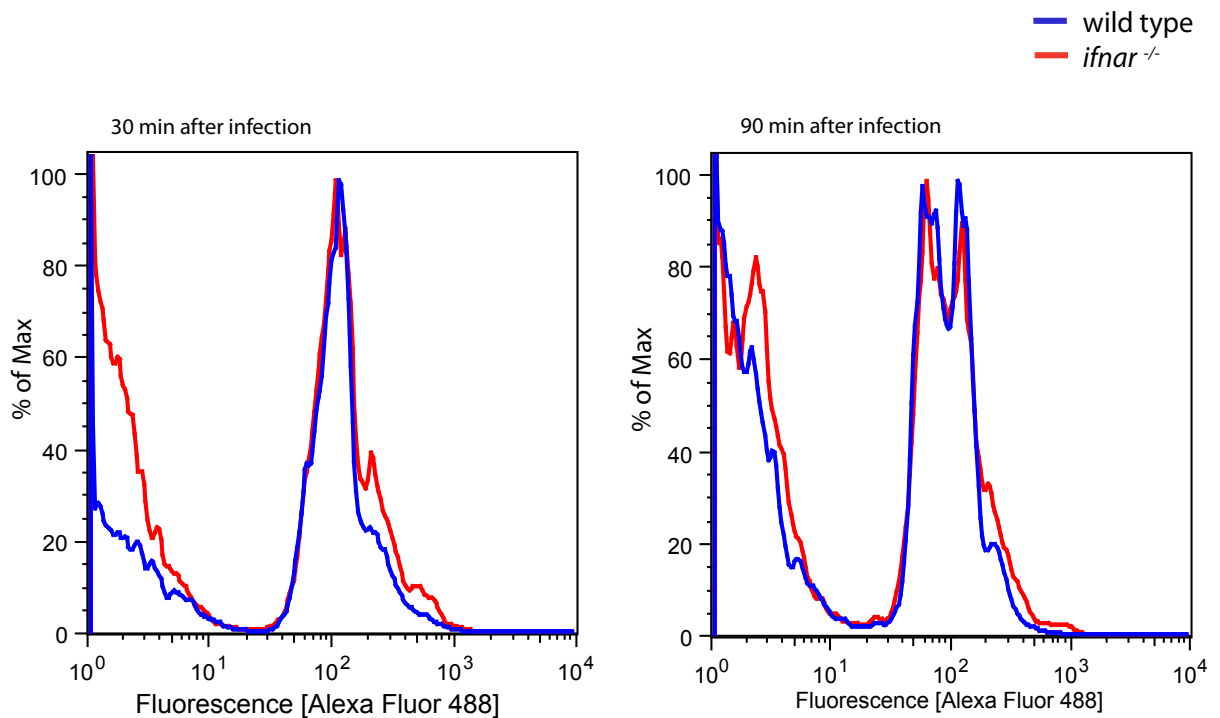
Figure 10. FACS analysis of WT vs. *Ifnar⁻ᐟ⁻* BMDCs using Alexa Fluor 488 stained *C. glabrata*

Phagocytic uptake was determined using FACS analysis with infected BMDCs 30 and 90 minutes after infection. Analysis was carried out comparing WT (blue) and *Ifnar⁻ᐟ⁻* (red) BMDCs. Uptake of fluorescently stained *C. glabrata* is displayed as an increase of fluorescence.
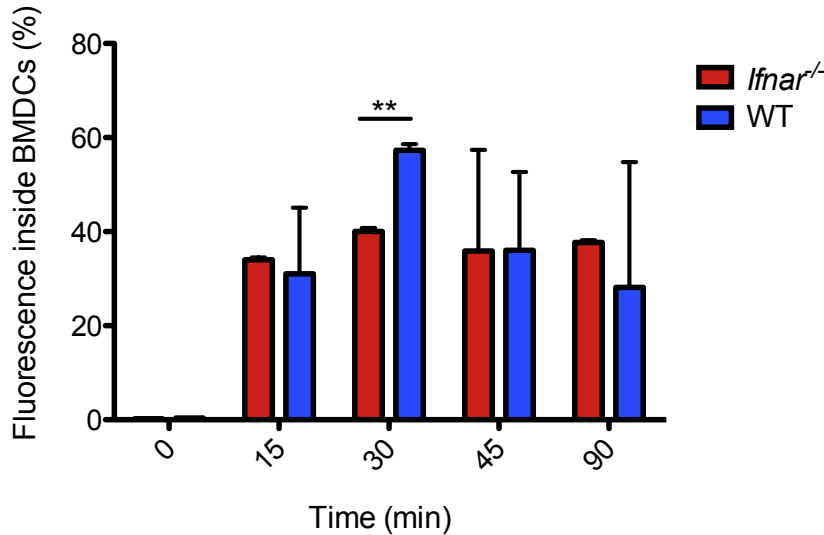
Figure 11. FACS analysis of the uptake of *C. glabrata* by BMDCs

Uptake of Alexa Fluor 488 stained *C. glabrata* is determined by the fluorescent signal inside BMDCs. The percentage of measured fluorescence inside the cells is given.

3.3 Isolation and quality control of the RNA used for sequencing

For the preservation of RNA, we performed an interaction between BMDMs and *C. glabrata* in a time - resolved manner. Hence, four independent biological mouse replicates of each condition (wild type and *Ifnar1$^{-/-}$*) and 5 independent replicates of *C. glabrata* served as samples. Since *C. glabrata* is a persistent pathogen we chose to perform a long - term infection. Therefore, the following time points were chosen: 1 hour, 2 hours, 6 hours and 24 hours. In addition, uninfected controls (0 hours) of each biological replicate and Candida (Candida only) were obtained. We conserved small, but sufficient amounts of RNA, ranging between 650 and 4550 ng of total RNA. The quality of the RNA was determined using an Agilent Bioanalyzer, which provides a so called RNA integrity number (RIN). RIN numbers can rang between 1 and 10, with 1 representing the lowest quality and 10 being the highest. In addition, it gives you an RNA gel picture and an elecropherogram image of your sample. In general it is said, that RNA with a RIN number lower than 6 is not suitable for sequencing, due to the high amounts

of degraded RNA. One of our replicates was completely degraded (replicate 1) and was therefore excluded from any further experiments. Interestingly, we saw that the software had difficulties in determining the RIN numbers for *C. glabrata* RNA. We reasoned that the software was set to identify mammalian RNA. However, Candida 28S RNA is smaller than mammalian. Therefore the software cannot identify it as 28S RNA, but marks it as degradation. Most of our RNA samples showed a RIN number higher than 7. The RIN numbers of 2 representative replicates and the *C. glabrata* only controls are shown in Table 1. One representative RNA gel figure of the samples WT2 0, WT2 1, WT2 2, WT2 6 and WT2 24 is shown (Figure 12).

sample	RIN number	sample	RIN number
WT2 0	9,8	WT3 0	9
WT2 1	9,4	WT3 1	9,4
WT2 2	8,5	WT3 2	9,3
WT2 6	8,8	WT3 6	9,5
WT2 24	9,2	WT3 24	9,5
Ifnar2 0	7,4	Ifnar3 0	8,5
Ifnar2 1	9	Ifnar3 1	8,8
Ifnar2 2	8,1	Ifnar3 2	8,9
Ifnar2 6	9,7	Ifnar3 6	9,4
Ifnar2 24	8,9	Ifnar3 24	8,8
Cg 1	10	Cg 3	8,6
Cg 2	9,6	Cg 4	N/A
		Cg 5	N/A

Table 1. RNA samples and corresponding RIN numbers of replicates 1 and 2, and 5 Candida only samples

The table represents the RIN numbers obtained for each indicated replicate and sample.
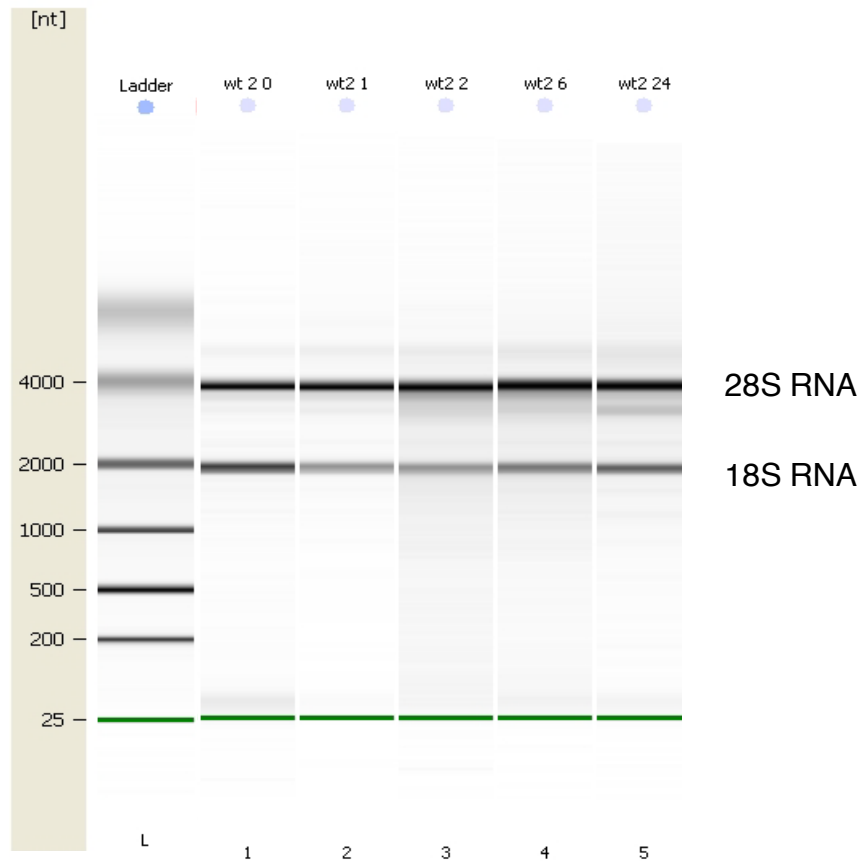
Figure 12. Bioanalyzer RNA gel picture of the samples WT2 0, WT2 1, WT2 2, WT2 6 and WT2 24

Indicated samples were quality checked using an Agilent Bioanalyzer. The figure shows the ladder, the 28S RNA and the 18S RNA for indicated samples.

In order to determine the best conditions for the sequencing, we decided to perform a pilot experiment using only one replicate of each condition including two Candida only samples. Therefore we chose the following samples for sequencing:

WT2 0	Ifnar2 0
WT2 1	Ifnar2 1
WT2 2	Ifnar2 2
WT2 6	Ifnar2 6
WT2 24	Ifnar2 24
Cg 1	
Cg 2	

3.4 Sequencing results

Our samples were sequenced at the CSF NGS Unit (Vienna, Austria) (csf.ac.at). The RNA Seq was carried out using True Seq sample preparation on an Illumina HiSeq 2000 (Illumina). We obtained 50bp long, single-end sequenced reads.

3.4.1 Quality control

We obtained a total amount of >115 million reads. Using the tool FastQC, we could detect a good per base quality throughout all samples. Good per base qualities are indicated by Phred Scores, which can range from 0 to 40, with 40 being the highest quality. Most commonly, Phred Scores smaller than 20 are considered to be "bad quality". Therefore, we discarded reads with a Phred Score smaller than 20. One representative picture of a FastQC report is shown in Figure 13.
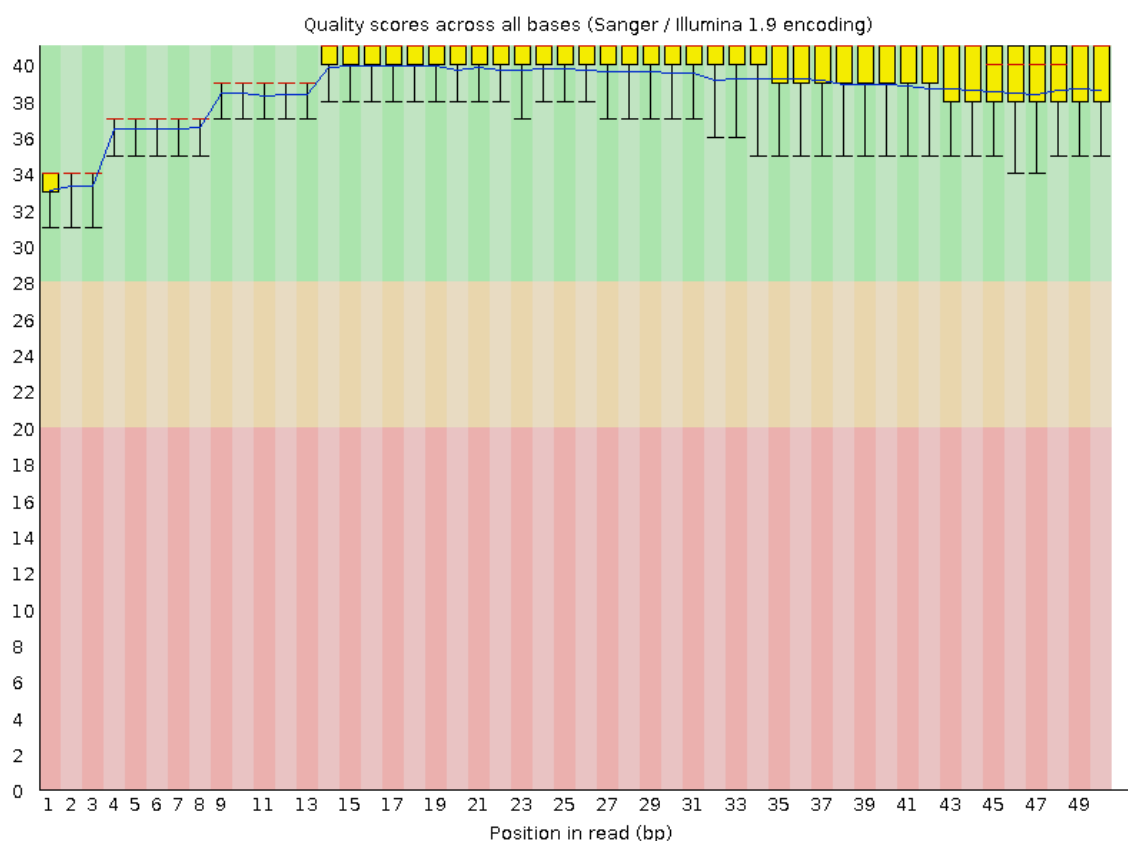
Figure 13. Per base sequence quality of one WT sample, time point 0

Phred Scores are obtained using the tool FastQC. The x - axis indicates the position of the base in the read. The Phred Score is shown on the y - axis.

3.4.2 Determining the amount of rRNA contamination in our samples

Before analyzing the sequencing results, we wanted to determine the amount of ribosomal RNA (rRNA) contamination in our samples, since this can be a disturbing factor during further analysis. Therefore we first mapped our sequence reads to the ribosomal RNA of mouse and Candida (Table 2).

| | total reads | mouse rRNA refernce | | | C. glabrata rRNA reference | | |
		mapped	unmapped	% mapping	mapped	unmapped	% mapping
Cg1	1838891	482806	1356085	26.3	974980	863911	53.0
Cg2	1226082	281052	945030	22.9	543603	682479	44.3
ifnar2_0	11501649	511032	10990617	4.4	183438	11318211	1.6
ifnar2_1	7571412	626050	6945362	8.3	490473	7080939	6.5
ifnar2_2	9023383	810934	8212449	9.0	729276	8294107	8.1
ifnar2_6	11500775	1849553	9651222	16.1	1080751	10420024	9.4
ifnar2_24	8900821	1641912	7258909	18.4	1725805	7175016	19.4
wt2_0	12250452	673580	11576872	5.5	288222	11962230	2.4
wt2_1	14138080	799637	13338443	5.7	404673	13733407	2.9
wt2_2	8643100	833466	7809634	9.6	697286	7945814	8.1
wt2_6	15080420	2385083	12695337	15.8	1299013	13781407	8.6
wt2_24	11562138	3186082	8376056	27.6	2141631	9420507	18.5

Table 2. Sequence reads mapping to rRNA from both mouse and Candida

The table shows total reads obtained during sequencing, and the amounts of reads that map and do not map to the rRNA of each individual respectively. The percentage of reads mapping to the reference is indicated.

Interestingly, we saw that Candida RNA mapped to its rRNA to a greater extent when compared to mouse mappings. This is probably due to the fact that the rRNA depletion kit we used is specialized to mammalian RNA, therefore not being able to adequately remove rRNA from the Candida samples. We also noticed that the amount of sequence reads mapping to rRNA increases over time. This makes perfectly sense, considering the fact, that *C. glabrata* is still growing. Therefore, the sample that has been taken after 24 hours of infection will contain considerably higher amounts of Candida RNA and therefore also more sequence reads mapping to rRNA.

We detected notable amounts (1,6% and 2,4%) of sequence reads mapping to Candida rRNA in the uninfected controls, which should not contain Candida RNA. Since rRNA consists of highly homologous regions, we assume that homologous sequences of mouse rRNA mapped to the genome of *C. glabrata*. This effect was

even more apparent when observing Candida only RNA mapping to mouse rRNA (26,3% and 22,9%). To circumvent this problem, we decided to map our sequence reads to a concatenated version of both rRNA reference files (Table 3). This way, we avoided double mappings of homologous regions.

		merged rRNA reference		
	total reads	mapped	unmapped	% mapping
Cg1	1838891	985561	853330	53.6
Cg2	1226082	548755	677327	44.8
ifnar2_0	11501649	522221	10979428	4.5
ifnar2_1	7571412	782537	6788875	10.3
ifnar2_2	9023383	1053625	7969758	11.7
ifnar2_6	11500775	2041429	9459346	17.8
ifnar2_24	8900821	2352827	6547994	26.4
wt2_0	12250452	700538	11549914	5.7
wt2_1	14138080	873459	13264621	6.2
wt2_2	8643100	1045362	7597738	12.1
wt2_6	15080420	2537565	12542855	16.8
wt2_24	11562138	3601627	7960511	31.2

Table 3. Sequence reads mapping to a concatenated file merged from mouse rRNA and Candida rRNA

This table again shows the amount total reads obtained during sequencing, and the reads that map and do not map to the merged rRNA reference. The percentage of reads mapping to the reference is indicated.

When mapping the sequence reads to a concatenated version of both rRNA references, we can see, that the numbers of mapped sequence reads are smaller than the sum of reads mapped only to the single rRNA references. This indicates that mapping to the concatenated version reduces the amount of falsely positive mapped reads.

3.4.3 Sequence reads mapping to the total genome reference

To see whether we obtained sequence reads that map to the whole genome reference, we mapped our sequence reads to the genomes of both organisms (Table 4). Since we discovered during the rRNA mapping, that mapping to single references can be problematic, we mapped our reads again to a concatenated version of the genomes (Table 5).

		mouse genome reference			C. glabrata genome reference		
	total reads	mapped	unmapped	% mapping	mapped	unmapped	% mapping
Cg1	1838891	461257	1377634	25.1	1634338	204553	88.9
Cg2	1226082	363144	862938	29.6	1089467	136615	88.9
ifnar2_0	11501649	10177664	1323985	88.5	1649205	9852444	14.3
ifnar2_1	7571412	5636287	1935125	74.4	1886623	5684789	24.9
ifnar2_2	9023383	5911573	3111810	65.5	2411606	6611777	26.7
ifnar2_6	11500775	8654939	2845836	75.3	2914751	8586024	25.3
ifnar2_24	8900821	5333204	3567617	59.9	4087188	4813633	45.9
wt2_0	12250452	10226120	2024332	83.5	1771685	10478767	14.5
wt2_1	14138080	12529517	1608563	88.6	2612527	11525553	18.5
wt2_2	8643100	6707216	1935884	77.6	1662431	6980669	19.2
wt2_6	15080420	11766245	3314175	78.0	3222467	11857953	21.4
wt2_24	11562138	7280859	4281279	63.0	4155038	7407100	35.9

Table 4. Sequence reads mapping to the mouse and Candida genomes

Shown are the total reads obtained during sequencing, and the amounts of reads that map and do not map to the total RNA of each individual respectively. The percentage of reads mapping to the references is indicated.

	merged genome reference			
	total reads	mapped	unmapped	% mapping
Cg1	1838891	1674970	163921	91.1
Cg2	1226082	1154584	71498	94.2
ifnar2_0	11501649	10310937	1190712	89.6
ifnar2_1	7571412	6448060	1123352	85.2
ifnar2_2	9023383	7005096	2018287	77.6
ifnar2_6	11500775	9833072	1667703	85.5
ifnar2_24	8900821	7420899	1479922	83.4
wt2_0	12250452	10439840	1810612	85.2
wt2_1	14138080	12939853	1198227	91.5
wt2_2	8643100	7269048	1374052	84.1
wt2_6	15080420	12772508	2307912	84.7
wt2_24	11562138	9448985	2113153	81.7

Table 5. Sequence reads mapping to a concatenated file merged from mouse and Candida genomes

This table shows the reads that map and do not map to the merged total genome reference. The percentage of reads mapping to the reference is indicated.

We were surprised to see that up to ~23% of the reads could not be mapped to the concatenated genome, therefore not mapping to any of the reference sequences. Reasons for this effect could be sequencing artefacts, polymorphic sequences or very variable regions, for example.

3.4.4 Coverage

Coverage is defined as the number of times each single nucleotide had been sequenced. A high coverage indicates, that the chance of having unsequenced areas in the genome is small[89]. A successful sequencing experiment should have a coverage at least higher than 20. Our samples reached a coverage between 5,3 and 10,5 (Table 6).

	Coverage
Cg1	9.19
Cg2	6.13
ifnar2_0	9.37
ifnar2_1	5.30
ifnar2_2	6.32
ifnar2_6	8.05
ifnar2_24	6.23
wt2_0	9.98
wt2_1	9.90
wt2_2	6.05
wt2_6	10.56
wt2_24	8.10

Table 6. Coverage obtained during RNA Seq experiment

The table indicates the coverage for each sample during sequencing. Note that the coverage is quite small due to the experimental setup.

3.4.5 Differential gene expression

To determine differentially gene expression, we used the R package DESeq. This tool offers the possibility of analyzing data that is not available in replicates.

We identified 244 genes differentially expressed in murine samples over time. In contrast, 510 differentially expressed genes were found in *C. glabrata* samples.

Comparing wild type and *Ifnar1*^{-/-} conditions, we detected 193 genes that were differentially expressed in at least one time point in mouse between WT and *Ifnar1*^{-/-}. 9 genes were differentially expressed in at least one time point in *C. glabrata* when infecting *Ifnar1*^{-/-} BMDCs compared to WT BMDCs

3.4.6 Integrative genomics viewer

To visualize differential gene expression, we choose the integrative genomics viewer (igv). Two representative pictures of differentially expressed genes are shown. One of them is IRF7[90], a gene product that is dependent on type I IFN signaling, since it is located downstream of the IFNAR (Figure 14). As can be seen, IRF7 shows a strong expression after 6 hours of infection in the wild type. In contrast, a negligible amount of reads can be found in the *Ifnar1*^{-/-} BMDCs. As a comparison, we chose a gene that is independent of type I IFN signaling, namely Interleukin - 1 beta (IL-1β)[91] (Figure 15). IL-1β is an important cytokine in triggering the inflammatory response and is therefore strongly expressed 6 hours after infection. The expression levels of IL-1β in wild type and *Ifnar1*^{-/-} BMDCs are marginally different.
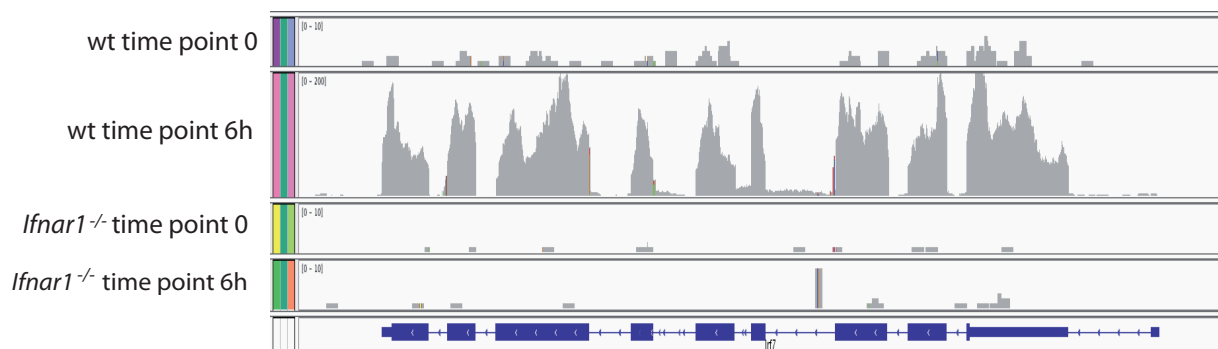
Figure 14. Expression of IRF7 is drastically reduced in the *Ifnar1*^{-/-} BMDCs

Differential gene expression of IRF7 between wild type BMDCs and *Ifnar1*^{-/-} BMDCs after 6 hours of infection was visualized using igv.
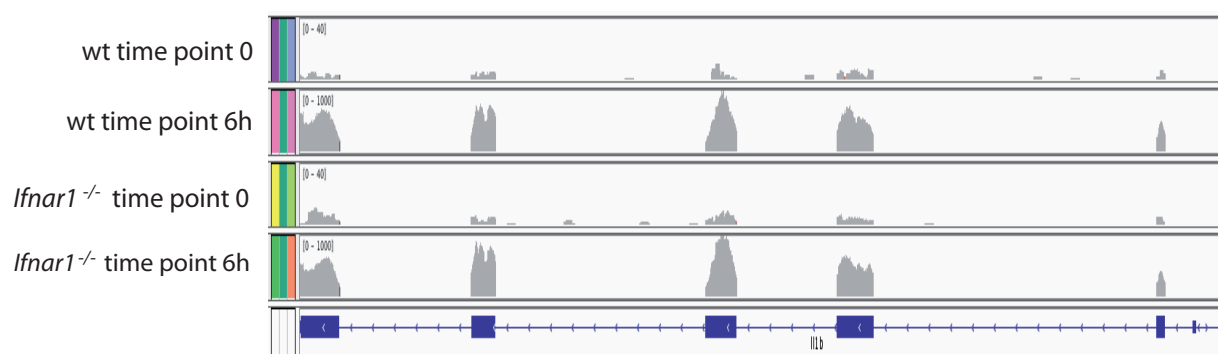
Figure 15. Expression of IL1-β is not affected by the loss of the type I IFNs receptor

Differential gene expression of IL1-β between wild type BMDCs and *Ifnar1*^{-/-} BMDCs after 6 hours of infection was visualized using igv.

3.4.7 Discovery of gene categories in *C. glabrata* using gene ontology (GO) terms

In high throughput experiments, genes can be categorized by their gene ontology (GO) terms in order to make it easier to visualize and analyze enrichment of certain pathways or biological processes in experimental conditions[92]. We used FungiFun to identify GO terms in *C. glabrata* that are important during infection (https://elbe.hki-jena.de/fungifun/fungifun.php). This tool allows one to perform gene set enrichment analysis by clustering genes based on their GO terms[93]. Gene set enrichment analysis enables interpretation of large gene expression data by assembling genes based on common biological function, location on the chromosome and regulation[94]. FungiFun identifies sets of genes which are over- or underrepresented under certain conditions. Figure 16 represents GO terms which are enriched in *C. glabrata* one hour after infection. As can be seen, numerous gene clusters are present, indicating the complexity of interacting genes and proteins during infection. Table 7 gives a complete list of enriched GO terms in *C. glabrata* one hour after infection.

Legend:
- plasma membrane
- fungal-type cell wall
- mitochondrial respiratory chain complex III
- hydrogen peroxide catabolic process
- aerobic respiration
- lysine biosynthetic process
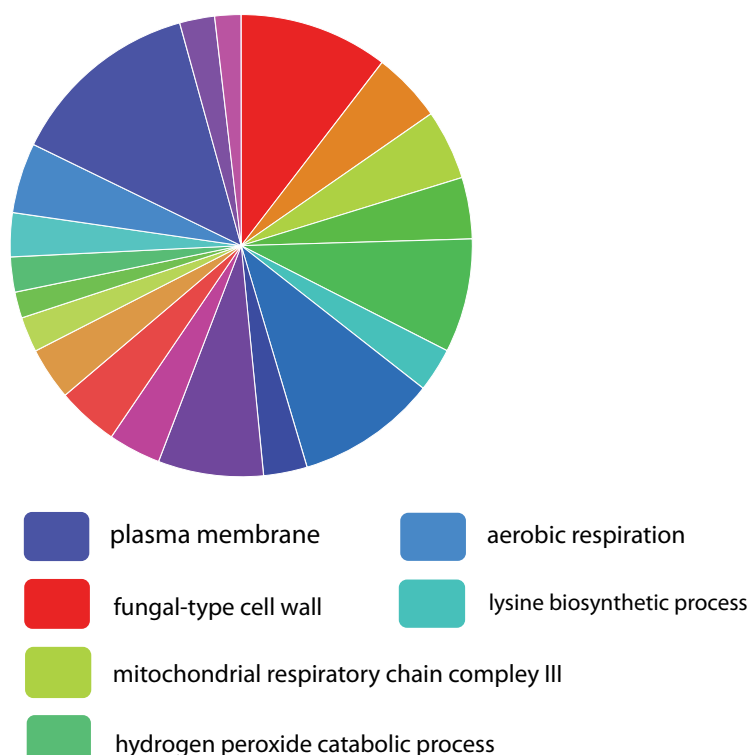
Figure 16. GO term enrichment of differentially expressed genes in *C. glabrata*

This pie chart shows the enrichment of GO terms that were overrepresented in *C. glabrata* one hour after infection. Different colors indicate different gene categories. Six highly overrepresented

categories are named in the image description. A complete list of enriched GO terms can be found in Table 7.

| GO ID	GO name	Exact p-value	# genes / input
GO:0009277	fungal-type cell wall	2.4306e-12	17 / 154
GO:0006122	mitochondrial electron transport, ubiquinol to cytochrome c	1.433e-11	8 / 154
GO:0005750	mitochondrial respiratory chain complex III	1.433e-11	8 / 154
GO:0008121	ubiquinol-cytochrome-c reductase activity	9.6842e-11	7 / 154
GO:0009986	cell surface	1.9897e-8	13 / 154
GO:0019878	lysine biosynthetic process via aminoadipic acid	9.811e-8	5 / 154
GO:0031505	fungal-type cell wall organization	5.5863e-7	16 / 154
GO:0000786	nucleosome	8.7452e-7	5 / 154
GO:0005576	extracellular region	1.6515E-06	12 / 154
GO:0006334	nucleosome assembly	4.3676E-06	6 / 154
GO:0030446	hyphal cell wall	0.000005187	7 / 154
GO:0030445	yeast-form cell wall	0.00001275	6 / 154
GO:0006526	arginine biosynthetic process	0.000019932	4 / 154
GO:0042744	hydrogen peroxide catabolic process	0.000022003	3 / 154
GO:0000105	histidine biosynthetic process	0.000038989	4 / 154
GO:0005199	structural constituent of cell wall	0.000039937	5 / 154
GO:0009060	aerobic respiration	0.000041188	8 / 154
GO:0005886	plasma membrane	0.000063735	22 / 154
GO:0046658	anchored component of plasma membrane	0.000068641	4 / 154
GO:0016597	amino acid binding	0.000086185	3 / 154
GO:0055114	oxidation-reduction process	0.000090163	14 / 154
GO:0005751	mitochondrial respiratory chain complex IV	0.00035653	4 / 154
GO:0004553	hydrolase activity, hydrolyzing O-glycosyl compounds	0.00070826	3 / 154
GO:0009922	fatty acid elongase activity	0.00079022	2 / 154
GO:0004475	mannose-1-phosphate guanylyltransferase activity	0.00079022	2 / 154
GO:0042450	arginine biosynthetic process via ornithine	0.00079022	2 / 154
GO:0006037	cell wall chitin metabolic process	0.00079022	2 / 154
GO:0003984	acetolactate synthase activity	0.00079022	2 / 154
GO:0005948	acetolactate synthase complex	0.00079022	2 / 154
GO:0004410	homocitrate synthase activity	0.00079022	2 / 154
GO:0016757	transferase activity, transferring glycosyl groups	0.00079022	2 / 154
GO:0004190	aspartic-type endopeptidase activity	0.00084943	4 / 154
GO:0004129	cytochrome-c oxidase activity	0.00084943	4 / 154
GO:0005759	mitochondrial matrix	0.00089929	7 / 154
GO:0020037	heme binding	0.0020709	4 / 154
GO:0030428	cell septum	0.0020709	4 / 154
GO:0043935	sexual sporulation resulting in formation of a cellular spore	0.0022812	3 / 154
GO:0006123	mitochondrial electron transport, cytochrome c to oxygen	0.0022812	3 / 154
GO:0009082	branched-chain amino acid biosynthetic process	0.0023267	2 / 154
GO:0009298	GDP-mannose biosynthetic process	0.0023267	2 / 154

Table 7. Complete list of GO terms overrepresented in *C. glabrata* during infection

This table indicates the GO ID and the GO names that are enriched one hour after infection. According to the FungiFun description, P - values give the probability of finding the same number of hits with a random gene list. P - values are calculated by the software using Fisher's exact test. In addition, for each GO term, the numbers of genes out of total input genes are shown.

3.4.8 Validation of selected gens obtained by sequencing

Due to the huge amount of data obtained by massive parallel (deep) RNA sequencing and the limited amount of time, we were obviously not able to validate all the genes that were differentially expressed. Instead, we decided to focus on the analysis of differential gene expression in *C. glabrata*. After doing some research, we ended up with a list of selected genes that were of interest to us (Table 8). Some of those genes were uncharacterized. Therefore, the decision of whether they are "interesting" or not was made by their homologies to other yeast species, like *C. albicans* or *S. cerevisiae*. A short summary of the functions of selected genes is shown in Table 8.

GENE	FOLD CHANGE					
	wt1	wt2	wt6	wt24	Type	*S. c.* homologue
CAGL0E01771g	3.39	2.97	2.75	1.22	ORF|Uncharacterized	NA
CAGL0F07601g	4.80	2.26	3.33	3.69	ORF|Verified	CWP2
CAGL0G04851g	3.37	1.95	2.05	1.82	ORF|Verified	SUR4
CAGL0G05896g	2.51	3.46	3.29	1.80	ORF|Uncharacterized	DSE2
CAGL0G09449g	4.13	4.48	4.44	2.66	ORF|Verified	CRH1
CAGL0H02255g	3.32	3.14	2.91	1.73	ORF|Uncharacterized	RSN1
CAGL0I06160g	3.59	2.72	3.60	3.63	ORF|Verified	CIS3
CAGL0M03773g	4.49	4.70	6.12	5.82	ORF|Uncharacterized	TOS6

Table 8. Genes selected for validation due to their fold change identified by RNA Seq

The table shows selected genes chosen for validation, the fold change in wild type DCs for each indicated time point, the type of gene (ORF) and its homologues to *S. cerevisiae* (*S. c.*) genes. *S. cerevisiae* data was obtained by the Candida Genome Database (http://www.candidagenome.org/).

Due to the fact, that none of those genes showed differential expression between wild type and *ifnar*^{-/-} (data not shown), validation was carried out using only wild type BMDCs. Using quantitative real - time polymerase chain reaction (qPCR), we were further able to validate differential gene expression in three of the selected genes: *CAGL0H02255g, GAGL0G09449g* and *GAGL0I06160g* (Figure 17 - Figure 19). *CAGL0G09449g* and *CAGL0I06160g* are GPI anchored proteins. *CAGL0I06160g* has a homologous gene in *S. cerevisiae* called *CIS3* and most likely encodes a homologue of the γ-glutamyltransferase[95], a protein, that is important in the vacuolar transport and the metabolism of glutathione in yeast[96].

CAGL0G09449g has a *S. cerevisiae* homologue called *CRH1*, which encodes a protein that is important in chitin linkage in budding yeast[97]. The third gene that was validated was *CAGL0H02255g*, which has one homologous gene in *S. cerevisiae*, called *RSN1. RSN1* is a membrane protein of unknown function, which has been associated with sodium pump function[98]. An overview of the functional properties of the other genes is given in Table 9.
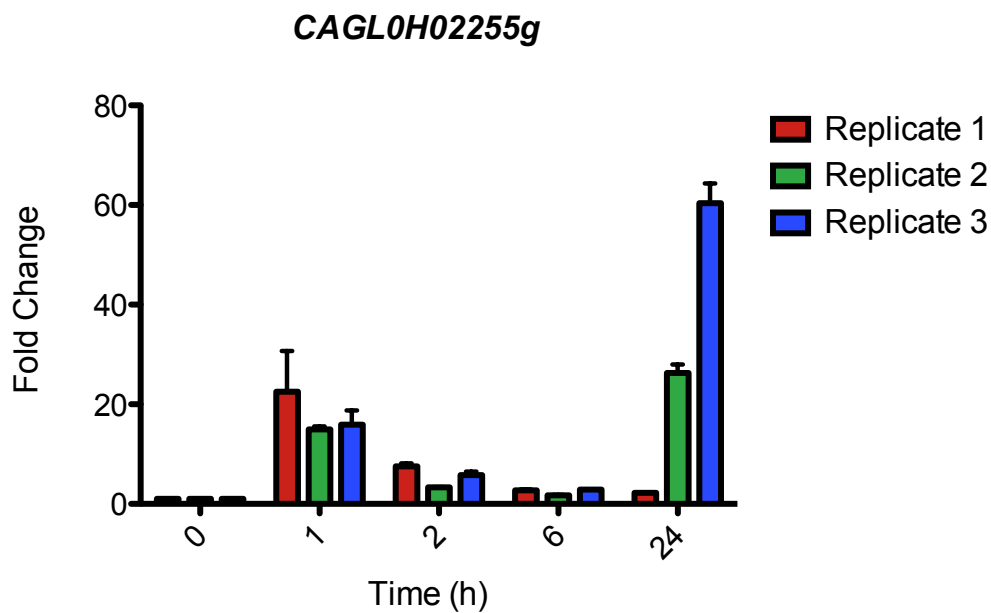
CAGL0H02255g

Figure 17. Fold change of *CAGL0H02255g* during interaction with BMDCs

qPCR was performed of three independent biological *C. glabrata* replicates after interaction with BMDCs over a time course of 24 hours. Fold changes were determined using changes in mRNA expression based on the expression levels of the house - keeping gene *Actin 1 (Act1).*
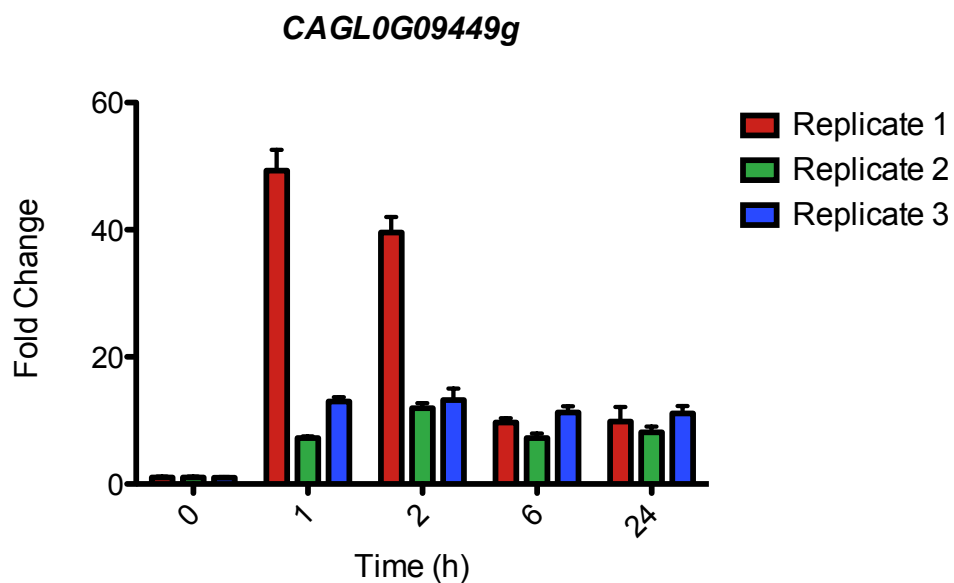
CAGL0G09449g

Figure 18. Fold change of *GAGL0G09449g* during interaction with BMDCs

qPCR was performed of three independent biological *C. glabrata* replicates after interaction with BMDCs over a time course of 24 hours. Fold changes were determined using changes in mRNA expression based on the expression levels of a house - keeping gene (*Act1*).
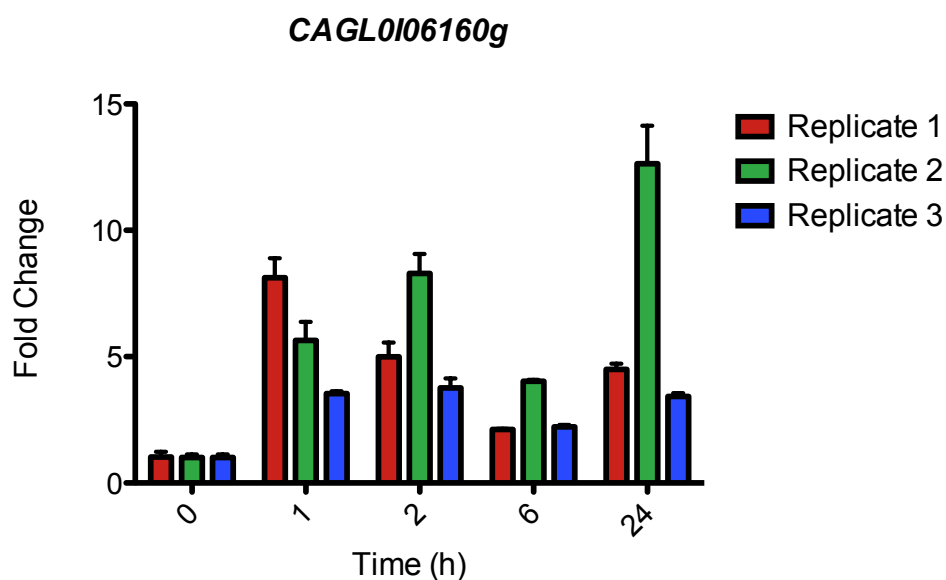
CAGL0I06160g

Figure 19. Fold change of *GAGL0I06160g* during interaction with BMDCs

qPCR was performed of three independent biological *C. glabrata* replicates after interaction with BMDCs over a time course of 24 hours. Fold changes were determined using changes in mRNA expression based on the expression levels of a house - keeping gene (*Act1*).

Gene	Description
CAGL0E01771g	Putative aspartic protease, predicted GPI - anchor, member of a YPS gene cluster that is required for virulence in mice, gene is downregulated in azole - resistant strain
CAGL0F07601g	Putative GPI - linked cell wall protein, involved in low pH resistance
CAGL0G04851g	Predicted fatty acid elongase involved in production of very long chain fatty acids for sphingolipid biosynthesis, mutants show reduced sensitivity to caspofungin and increased sensitivity to micafungin
CAGL0G05896g	Putative adhesin - like protein
CAGL0M03773g	Predicted GPI - linked adhesin - like protein

Table 9. Descriptions of genes that could not be validated using qPCR

Gene description data was obtained by the Candida Genome Database (http://www.candidagenome.org/).

3.5 Growth of *CAGL0H02255gΔ*, *CAGL0G09449gΔ* and *CAGL0I06160gΔ* in YPD

After validation, we wanted to perform experiments using knockouts of those genes. We obtained these knockouts from a large *C. glabrata* deletion library that was generated by our lab. The knockouts *CAGL0G09449gΔ* and *CAGL0I06160gΔ* were previously generated and published[41]. *CAGL0H02255gΔ* was previously generated by Istel et al., *in preparation*. To determine whether the validated mutants show altered growth compared to the wild type, a growth curve was generated in YPD at 30°C and 220 rpm. As can be shown in Figure 20, there was no significant difference in growth between any of the knockouts.
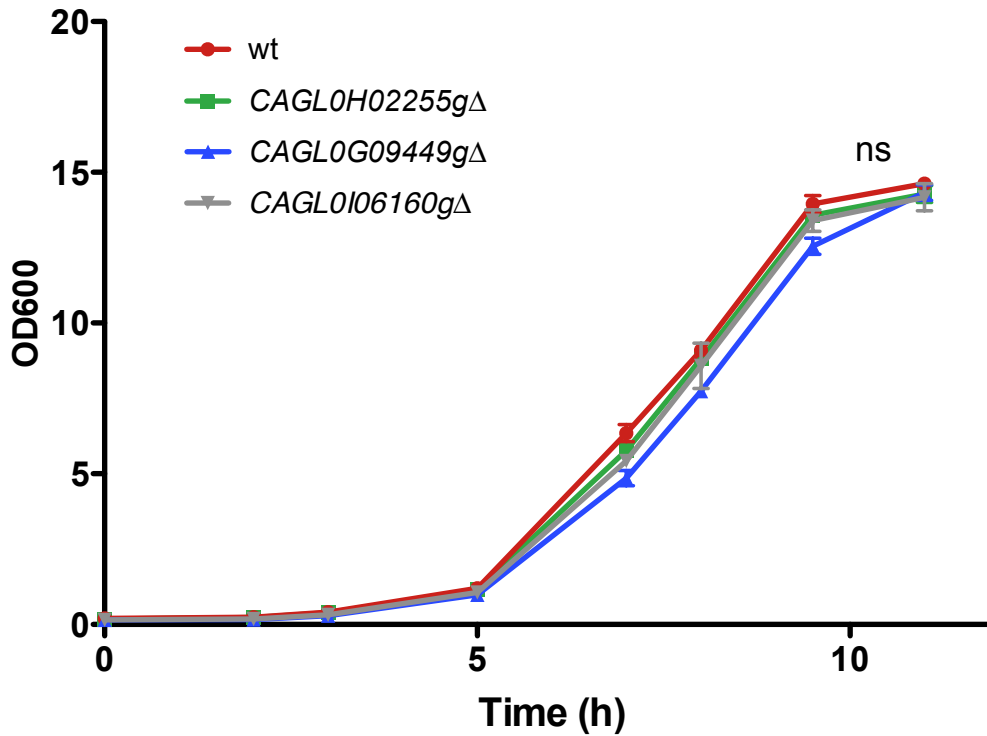
Figure 20. Growth of *CAGL0H02255gΔ*, *CAGL0G09449gΔ* and *CAGL0I06160gΔ* compared to the wild type

Growth of *C. glabrata* was determined in YPD at 30°C and 220 rpm. Statistical analysis was carried out using a one - way ANOVA and Tukey's post test. P - value > 0.05 is indicated by "ns".

3.6 Survival assay of *CAGL0H02255gΔ*, *CAGL0G09449gΔ* and *CAGL0I06160gΔ* in BMDCs

We further wanted to see whether our knockouts had a reduced survival rate during infection of BMDCs *in vitro*. Therefore, we differentiated BMDCs *in vitro* and infected them with wild type *C. glabrata* and the respective *C. glabrata* knockouts. The interaction covered a time course of 24 hours with samples being taken 2, 8 and 24 hours after infection. Indeed, we did see a significant difference in the survival of all *C. glabrata* knockouts after 8 hours of interaction with BMDCs (Figure 21). However, one has to be careful when interpreting this data, since there is a clear tendency of the wild type having higher CFUs in all time points compared to the knockouts. Additionally, the experiment was carried out using only 2 technical replicates. In

order to confirm these results, the experiment needs to be repeated using at least three independent biological replicates.
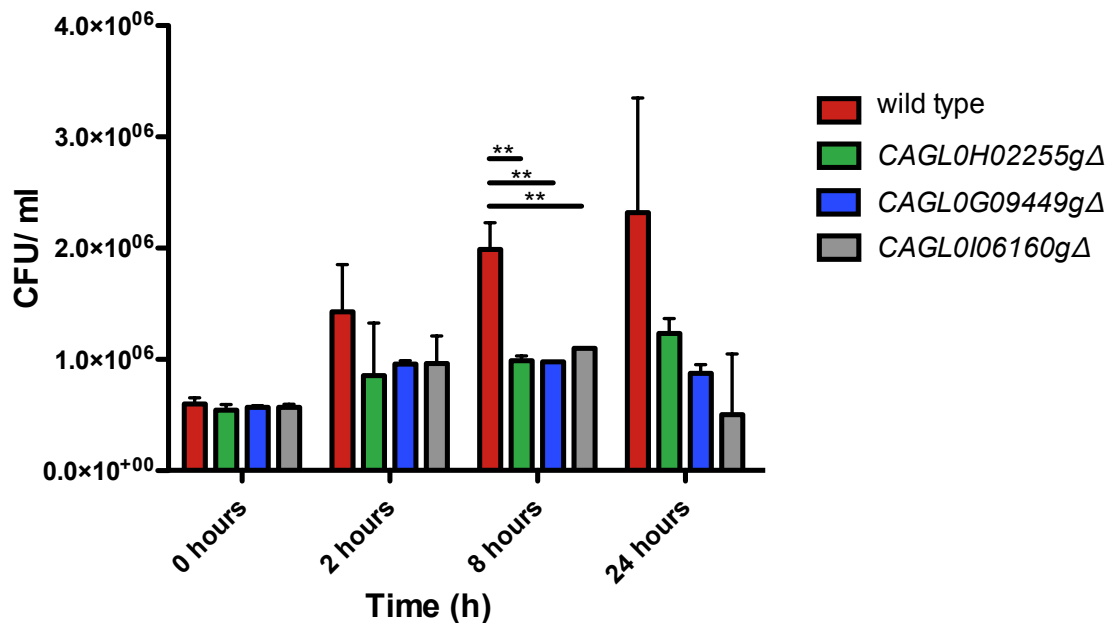
Figure 21. Survival assay of different *C. glabrata* knockouts during an interaction with BMDCs

Survival inside WT BMDCs was analyzed using *CAGL0H02255gΔ*, *CAGL0G09449gΔ* and *CAGL0I06160gΔ* during infection over a time course of 24 hours. Statistical analysis was carried out using a one - way ANOVA and Tukey's post test. P - value ≤ 0.01 is indicated by **.

3.7 Summary of the results

We identified differential expression of immune - related genes in murine BMDCs. Furthermore, a list of GO terms in *C. glabrata* was created to indicate the importance of gene categories. Additionally, we identified 3 novel genes in *C. glabrata,* that are assumed to be important during infection.

As a side project, we studied the effects of DMEM, which was supplemented with 10% FCS, Penicillin and Streptomycin, to the growth of *C. glabrata,* and identified temperature - dependent inhibition of fungal growth in supplemented DMEM.

4 Discussion

4.1 Growth of *Candida glabrata* in DMEM

During our studies, we discovered the complete lack of growth of *C. glabrata* in DMEM, which was supplemented with 10% FCS, Penicillin and Streptomycin at 30°C. We further discovered that the ability to grow in DMEM was improved when incubating at 37°C instead of 30°C. However, growth at 37°C was still weaker compared to growth in YPD, which was independent of temperature. We therefore asked ourselves which components of YPD and DMEM are responsible for growth of Candida and the factors that influence growth at certain temperatures.

YPD is a full media commonly used for the cultivation of yeast. It is composed of yeast - extract, peptone and dextrose, and allows the rapid growth of yeast due to its high abundance of sugar and proteins, thereby supplying the yeast with carbon and nitrogen. In addition, it contains vitamins and minerals. This media is optimized for yeast growth. Therefore, strong growth of *C. glabrata* is not surprising. DMEM on the other hand is intended to be used in cell culture. It contains high concentrations of glucose and glutamine, which supplies the mammalian cells with carbon and nitrogen. Additionally, our supplemented DMEM contains FCS. Serum is used due to its high concentration of growth factors and it provides the cells with a high amount of nutrients. However, FCS is an undefined product[99]. Therefore, it is impossible to determine the exact ingredients and, hence, predictions about its properties are difficult. Nevertheless, it is known that the presence of serum does influence the growth of other Candida species. *C. albicans*, for example, starts to form hyphae when exposed to serum[100]. Optimal hyphal growth is achieved when incubating the fungus at 37°C in combination with serum[101]. Since the formation of hyphae is an important virulence trait of *C. albicans*[6], it makes perfectly sense, that the presence of physiological, body - like conditions, induces hyphal growth. We asked ourselves, whether growth of *C. glabrata* at physiological conditions could

underlie comparable mechanisms. Reports suggest, that the presence of sterol in serum is an important virulence trait in *C. glabrata*[102,103]. However, exact mechanisms of how supplemented DMEM effects growth of *C. glabrata* are not yet understood. We believe that growth of *C. glabrata* might be inhibited in supplemented DMEM at 30°C, because of the physiological conditions of the medium itself. Therefore, raising the temperature to physiological, body - like temperatures positively contributes to growth. However, we are aware that growth of *C. glabrata* can also be impaired due to stress caused by the limited availability of nutrients.

4.2 The effects of rRNA and low coverage on sequencing data

One of the first steps during the analysis of the sequencing data was to determine the amount of rRNA contamination in our samples. Since we treated our RNA samples with an rRNA depletion kit prior to sequencing, we expected low amounts of reads mapping to rRNA. This was the case for murine RNA, with small amounts of rRNA contaminations (~5%). However, when looking at the Candida samples, we found up to 53% of the reads mapping to rRNA. As mentioned above, the high contamination with *C. glabrata* rRNA most likely results from an inability of the rRNA depletion kit to deplete non - mammalian rRNA. It has been shown that the presence of rRNA can disturb sequencing results by reducing the coverage of mRNA[79,104]. We were wondering whether high amounts of rRNA in our Candida samples would lead to poor results compared to mouse samples. However, Candida samples showed a similar coverage to the mouse samples (Table 6). This is most likely due to the fact that coverage is calculated in relation to the transcriptome length. Since the transcriptome length of *C. glabrata* is much smaller than the transcriptome length of mouse (~1/6 smaller) the effects of high numbers of reads mapping to rRNA are relatively small. However, we believe that problems can occur when analyzing mixed samples (Candida and mouse RNA mixed during infection). One issue about dual - species RNA Seq is the fact, that it is not possible to determine the amount of RNA per species prior to sequencing. Therefore, it is possible that

one species ends up exhibiting considerably higher amounts of RNA in one sample and hence, also reaching higher coverage. Enhancing the coverage can solve this problem. However, this is not always possible due to technical and financial limitations. Also, many groups are not able to repeat sequencing experiments over and over until finding the best conditions. Therefore, it is most important to be completely confident of what one wants to prove when planning RNA Seq experiments. Many different biological questions can be addressed by RNA Seq, and not all of the approaches demand the same conditions. For example, if one wants to investigate differentially gene expression, a low coverage might be enough, if the changes in gene expression are expected to be high. Although having a low coverage, differentially expressed genes can be detected under these circumstances. However, other approaches may need a higher coverage, for example the high - confident genotyping of individual genomes[105], or the detection of specific microRNAs during sequencing[106].

Low coverage was also an issue during our studies. We generally obtained a rather small coverage for our samples (Table 6). Since we planned this study as a pilot experiment we were satisfied with the results, although knowing that a low coverage can result in false negative results when analyzing differentially gene expression. This is due to the fact that genes with a low expression level will not produce enough reads to statistically differ from unexpressed genes. Although having identified many differential expressed genes in our data set, we believe that the coverage obtained during our experiment is not enough to provide us with the necessary amount of information. This can be seen not only by the coverage itself, but also by the fold changes of differential expressed genes. When looking at the fold changes of differential expressed Candida genes in Table 8, we see that none of the genes exhibits a higher fold change than ~6. We were surprised about this effect, since we expected higher fold changes for differentially expressed genes due to the infectious conditions. The effect became even more apparent when carrying out qPCRs for validation. We detected large differences in the fold changes obtained by qPCR when compared to the fold changes obtained by sequencing. For example, when looking at the differential

gene expression of *CAGL0H02255g* one hour after infection, we saw that qPCR data displays an average fold change of ~20, whereas sequencing reveals a fold change of 3,32. In addition, many genes that were determined differentially expressed when analyzing sequencing data, could not be validated by qPCR. Out of the tested genes, we were able to validate only three. We don't know exactly what caused this phenomenon. However, we think that the low coverage contributes to this effect, since we believe that the small amounts of reads are not sufficient to reveal the actual expression levels of the genes. Therefore, we assume that a low coverage may not only lead to false negative, but also to false positive results. However, since it has ben shown that false positive results only slightly follow from low coverage[107], we assume that this problem was rather caused due to a misalignment of reads[108].

Another phenomenon that we detected was the strong divergence between different replicates while validation using qPCR (Figure 17 - Figure 19). Although we cannot exactly know where this divergence results from, we believe that this problem may most likely arise from pipetting errors, errors during sample preparation or natural biological variances.

4.3 Working without replicates

We analyzed sequencing data that was not available in replicates. It is needless to say, that working without replicates is not the method of choice when determining biological mechanisms, since differences between samples can be caused by experimental and biological noise, rather than by different conditions. However, we have shown that successful pilot experiments in RNA Seq can be carried out by using only one replicate. We were able to detect differential gene expression und successfully validated data obtained by sequencing.

In order to analyze our data, we used the R package DESeq which offers the possibility to analyze data that is not available in replicates. Although conclusions drawn from this data is of limited reliability, it can be useful to deal with this kind of information. To keep it simple, DESeq determines differentially expression by

investigating whether variances between two conditions are higher than the variances inbetween replicates. If this is the case, variances between conditions are caused due to differentially expressed genes. If there are no replicates available, the program "fakes" a replicate by treating the different conditions like replicates. Instead of determining variances between replicates, it uses the mean of the variance between conditions as variance between replicates. This algorithm only works by assuming, that most genes in the data set will not be differentially expressed and therefore, won't significantly influence the mean variance. However, this approach will make the calculations more conservative[109]. Therefore, fewer genes will be detected as differentially expressed and the data will deliver false negative results.

Either way, unreplicated data will lead to false assumptions due to the complete lack of knowledge about the real biological variance between replicates[110]. When having to decide between a high coverage and a high number of biological replicates, opinions are divided. While some reports favor the usage of only one replicate with a high coverage[111], recent reports suggest the use of more replicates when having the option[112].

4.4 Enriched gene ontology (GO) terms and the identified differentially expressed genes

One of the major challenges with high - throughput methods is the huge amount of data obtained during analysis. To simplify this task, researchers have developed tools that enable one to look at specific categories of genes rather than analyzing single differentially expressed genes. These tools provide the possibility of designing an ontology which represents gene function or location on the chromosome, for example. One of the major advantages is the common and comprehensive identification of genes throughout different databases. Also, it simplifies research concerning homologous genes and functional aspects among different species. Genes can code for products with biologically different functions, for example by alternative splicing[113]. Therefore, it is important to being

able to compare homologous, orthologous and paralogous genes between species.

During our studies, we identified gene categories that were differentially expressed using GO terms. By using this tool, we could successfully detect biological functions in *C. glabrata* that were overrepresented during infection. One of the GO terms that were most overrepresented were related to the cell wall, the cell surface and the plasma membrane of the yeast. The cell wall is an important structural protection for the fungus and has been implicated to be important during host - fungus interactions. It helps the pathogen during adhesion and invasion, and is responsible for biofilm formation[114–116]. Therefore, an enrichment of cell wall - related genes makes perfectly sense and was expected by us.

Not much is known about the role of *C. glabratas* plasma membrane during infection. However, it is associated with virulence in *C. albicans* and its ability to adhere to the host cell via adhesins[117]. One of the gene groups that plays an important role during adherence are GPI - anchored proteins[114,118–120], which comprise more than 80% of all covalently linked cell wall proteins in *C. albicans*[121]. Two of the differentially expressed genes that we were able to identify during our studies are putative GPI - anchored protein, namely *CAGL0G09449g* and *CAGL0I06160g*. *CAGL0I06160g* has a homologous gene in *S. cerevisiae* called *CIS3*. *CIS3* is believed to encode a homologue of the γ-glutamyltransferase[95], a protein, that is important in the vacuolar transport and the metabolism of glutathione in yeast[96]. Recent reports suggest a pivotal role of vesicle - mediated transport in the virulence of *C. glabrata* by impairing the phagolysosomal maturation[122]. Therefore, it was interesting to us, whether the deletion of *CAGL0I06160g* attenuates virulence in *C. glabrata*. *CAGL0G09449g* has a *S. cerevisiae* homologue called *CRH1*, which encodes a protein that is important in chitin linkage in the cell wall of budding yeast[97]. The cell wall of *C. glabrata* is the first point of contact between the pathogen and the host cell and it is assumed to account to the pathogenicity of Candida species in general[123,124]. We suggest that the deletion of genes important in cell wall biogenesis could alter the virulence of *C. glabrata*, due to its role in adherence to the host cell.

The third gene that we were able to validate was *CAGL0H02255g*. *CAGL0H02255g* is an uncharacterized gene in *C. glabrata,* and has one homologous gene in *S. cerevisiae*, called *RSN1. RSN1* is a membrane protein of unknown function, which has been associated with sodium pump function, NaCl tolerance and vesicular transport transport[98]. *CAGL0H02255g* is located at the plasma membrane.

Further studies need to be carried out to identify the role of these genes during infection, and to draw conclusions about their function as putative virulence genes.

Although this is only speculation, we believe that the use of GO term enrichment may be more useful than the investigation of single genes, when working with only one replicate. This is due to the fact that many genes contribute to the enrichment of GO terms. The chance of having false positive or false negative results in many genes is simply smaller than the chance of having false results when looking at only one gene.

4.5 Outlook

We showed that RNA Seq is a powerful tool to determine differentially gene expression and GO term enrichment. It is important to provide data that is available in a good quality and in biological replicates. Since this study was intended to be a pilot experiment, the next step is to repeat the sequencing with biological replicates and settings that provide a higher coverage. We are confident to reveal even more information when analyzing such a data set and hope to create a network composed of interacting genes of both organisms during infection.

5 Materials and methods

5.1 Cell and yeast cultures

5.1.1 Isolation of murine bone marrow

8 - 12 week old mice were used for isolation of bone marrow. After killing, femurs and tibiae were removed, followed by the removal of any skin and flesh attached to the bone. The ends of the bone were then removed carefully with a scissor and bone marrow was obtained by flushing the bone with DMEM supplemented with 10% FCS and P/S using a small needle. The suspension was centrifuged for 7 minutes at 300 rcf and 4°C. The pellet was then treated with 0,5 ml/leg red cell lysis buffer. This buffer lyses erythrocytes in the sample due to its hypotonic characteristics causing influx of liquid into the erythrocytes and therefore lysis. Other cells are not as sensitive to hypotonic stress. Hence, they are unaffected by this buffer. The reaction was stopped after 2 minutes by adding 20 ml of DMEM supplemented with 10% FCS and P/S followed by centrifugation for 7 minutes at 300 rcf and 4°C. The cells were either brought into culture directly after isolation or prepared for freezing in liquid nitrogen. For freezing, 0,5 ml/leg of FCS complemented with 10% DMSO were added to the cell pellet and frozen away immediately at -80°C to avoid cytotoxic effects of DMSO. After one day at -80°C, frozen samples were transferred into liquid nitrogen where they were kept until usage.

Red cell lysis buffer: 8.3g/l NH_4Cl in 0.01M Tris-HCl buffer (pH 7,0)

5.1.2 Preparation and testing of J - conditioned media

A GM-CSF (granulocyte - macrophage colony stimulating factor) producing cell line (J558L) was plated in 10ml of DMEM supplemented with 10% FCS and P/S using 10 cm round cell culture treated dishes. After the cell line reached a semi - confluent stage, the cells were split to two 75 cm^2 cell culture - treated flasks filled with 80 ml of DMEM supplemented with 10% FCS and P/S each. After the cells became confluent, the media was taken off and the cells were washed gently with 20ml sterile PBS. Next, 100 ml of fresh non - supplemented DMEM (without any additives or antibiotics) were added to the flasks. The cells were incubated for several days until the media turned yellowish and most of the cells were dead. The media was then collected using a filter (Nalgene Filter Unit, Thermo Scientific) and stored at -20°C until testing.

For testing, bone marrow cells were plated in 6-well plates at a density of $5*10^5$ cells per well. 3 ml of supplemented DMEM with different concentrations of new J - conditioned media was used for testing (1%, 3%, 5%). As a control, cells were also grown in mDC media supplemented with 3% old J - conditioned media and in supplemented DMEM only (Figure 22).
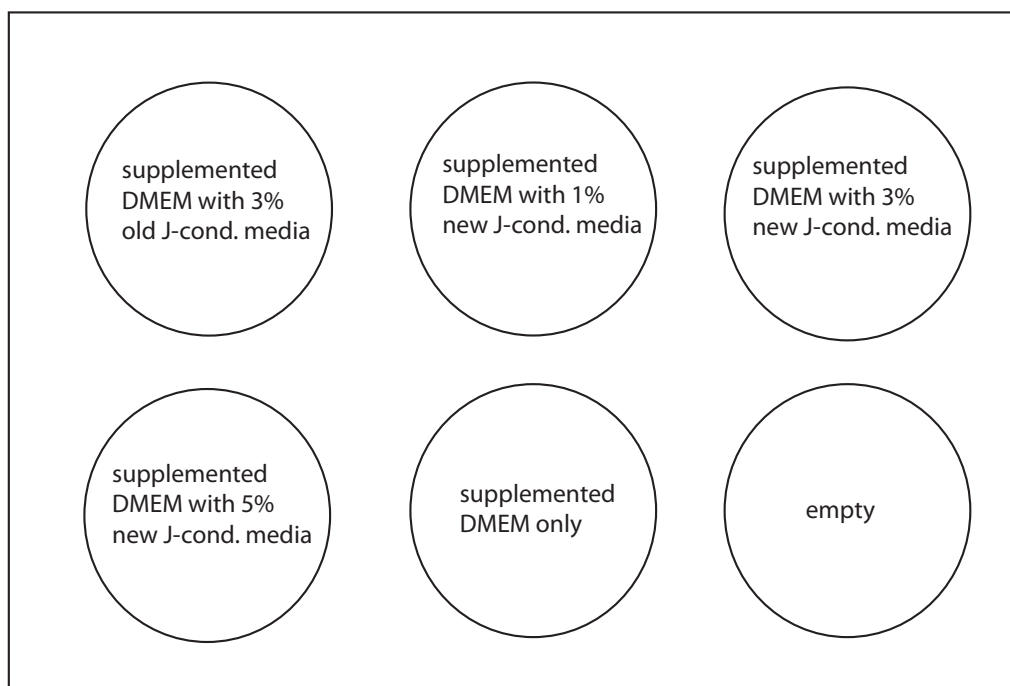
Figure 22. Setup of the 6 well plate used for testing new J - conditioned media

mDC media at different concentrations, and DMEM only respectively, were distributed in a cell culture treated 6 well plate (as indicated). Bone marrow cells were differentiated for 8 days until tested for quality by using fluorescently labeled antibodies on a FACS Calibur (BD Biosciences).

On day 3, 2 ml of each respective media was added. On day 8, cells were collected by gently flushing against the cell culture dish wall. The cells were centrifuged for 7 minutes at 300 rcf and 4°C and washed one time with ice cold PBS. For FACS analysis, cells were resuspended in 50 μl of FACS buffer (PBS + 1% FCS) and FC-gamma receptor block was carried out on ice for 5 minutes by adding 1 μl of anti - mouse CD16/CD32 antibody (0.5 mg/ml stock) (BD Biosciences) to the solution. Next, additional 50 μl of FACS buffer were added and cells were labeled with fluorescently labeled antibodies. Therefore, we added 1.5 μl of anti - mouse CD11c antibody (0.2 mg/ml) (BD Biosciences) and, additionally, 1.5 μl of anti - mouse F4/80 (0.2 mg/ml) (BioLegend) to optionally detect macrophages from the sample. After incubation on ice for 30 minutes in the dark, the sample was washed twice with PBS and resuspended in 400 μl FACS fix buffer (PBS + 1% FCS + 4% formaldehyde). The cells were then checked for fluorescence using a FACS Calibur (BD Biosciences). mDCs were defined as CD11c$^+$ and F4/80$^-$.

J558L cells: For the production of J - conditioned media, we used a cell line called L558L, which derived from murine B myeloma cells. They were transformed in order to produce recombinant GM-CSF, a growth factor that leads to the differentiation of mDCs from bone marrow-derived stem cells. GM - CSF has shown to be an effective stimulus to maintain the viability of mDCs, *in vitro.* In contrast, plasmacytoid dendritic cells are not obtained by the stimulation with GM - CSF[60].

5.1.3 Differentiation of murine bone marrow derived dendritic cells

Myeloid dendritic cells (mDCs) were differentiated using either frozen cells or cells directly obtained by flushing. Either way, cells were diluted in DMEM supplemented with 10% FCS and P/S. After centrifugation for 7 minutes at 300 rcf and 22°C, the supernatant was discarded and cells were plated in 8 ml/leg

mDC media using 10 cm round cell culture-treated dishes. The plates were incubated at 37°C in 5% CO_2 atmosphere. On day 3, 5 ml of mDC media was added to each dish. On day 7, dendritic cells were harvested by gently flushing against the cell culture dish wall with a pipette, while avoiding the detachment of adherent cells. After centrifugation for 7 minutes at 300 rcf and 22°C, the pellet was resuspended in 1 ml/leg mDC media. The cells were then ready to be counted and used for interaction studies. mDCs were differentiated from hematopoietic stem cells by the addition of granulocyte - macrophage colony stimulating factor (GM - CSF)[59].

5.1.4 Preparation of growth media for murine bone marrow derived dendritic cells

supplemented DMEM	450 ml Dulbecco's Modified Eagle Medium (DMEM) (GE Healthcare)
	50 ml heat inactivated fetal calf serum (FCS) (Sigma)
	100 U/ml penicillin (P)
	100 μg/ml streptomycin (S)
mDC media	supplemented DMEM as described above
	3% J - conditioned media

Growth media was prepared under sterile conditions and kept at 4°C until usage.

5.1.5 Preparation of culture media for Candida strains

liquid 1x YPD media:	10 g/l yeast extract (BD Biosciences)
	20 g/l bacto peptone (BD Biosciences)
	2% w/v glucose (Merck)

Yeast extract and bacto peptone were dissolved in 450 ml of ddH$_2$O, followed by autoclaving. 50 ml of autoclaved glucose (20% stock) were then added under sterile conditions.

YPD plates: 20 g/l yeast extract (BD Biosciences)

                     40 g/l bacto peptone (BD Biosciences)

                     4% w/v glucose (Merck)

Yeast extract and bacto peptone were dissolved in 200ml of ddH$_2$O, followed by autoclaving. 50 ml of autoclaved glucose (20% stock) were added after autoclaving under sterile conditions. This solution was mixed with sterile 4% (w/v) agar (BD Biosciences) to a total volume of 500 ml and poured into sterile round 9 cm dishes.

5.1.6 *C. glabrata* **and mouse strains used during our studies**

The *C. glabrata* strain ATCC2001 was used for all experiments. The knockouts *CAGL0G09449gΔ* and *CAGL0I06160gΔ* were previously generated and published[41]. *CAGL0H02255gΔ* was previously generated by Istel et al., in preparation. All knockouts derived from the *C. glabrata* ATCC2001 backup strain.

For all *in vitro* studies, BMDCs differentiated from 7 - 9 week old C57BL/6 mice were used. All animal - related work was carried out in accordance with the animal experimentation protocols approved by he Austrian law and were discussed and approved through the University of Veterinary Medicine Vienna institutional ethics committee.

5.1.7 Preparation of *Candida glabrata* culture for interaction with mouse bone marrow derived dendritic cells

C. glabrata was streaked out on YPD plates and incubated at room temperature until colonies were visible. A single colony of *C. glabrata* was then inoculated in 5 ml 1x YPD and incubated at 30°C and 220 rpm over night. A small amount of the over night culture was then transferred to 50 ml of 1x YPD and incubated at 30°C and 220 rpm until the sample reached an OD_{600} of ~1. The sample was then transferred to a 50 ml falcon tube and centrifuged for 5 minutes at 3000 rpm and 22°C. The pellet was washed two times with 50 ml PBS and finally resuspended in 10 ml PBS. The number of cells was determined using a CASY cell counter (Roche).

5.1.8 Interaction of mDCs and *C. glabrata* for RNA Sequencing

After harvesting, the cells were counted on a CASY cell counter (Roche). $3 * 10^6$ of mDCs were transferred to 6 cm round cell culture-treated dishes. After one day, cells were infected with *C. glabrata* at a multiplicity of infection (MOI) of 1:2 (BMDCs:Candida), meaning that 2 times the amount of Candida cells were used for the interaction ($6 * 10^6$). At indicated time points, cells and Candida were removed from the plate using 175 μl of RNA lysis buffer (Promega) by roughly scraping them from the cell culture dish. The cell lysate was stored at -80°C until RNA isolation was performed (see 4.2.1.).

5.1.9 Growth curve generation of *C. glabrata*

Growth curves of *C. glabrata* and *C. glabrata* knockouts were generated by diluting an overnight culture of Candida with either YPD or DMEM to an OD_{600} of 0,2. The culture was incubated at 30°C at an rpm of 220 and growth was determined using photospectrometry (U-2800 Spectrophotometer, Hitachi) at indicated time points, until the culture reached a stationary phase. Alternatively,

growth was determined using cell culture - treated dishes and incubation at 37°C or 30°C without rotation. Growth curve analysis was performed using at least 3 biological replicates.

5.1.10 Phagocytosis assay of *C. glabrata* with DCs

C. glabrata was inoculated to an OD_{600} of 1 for the next day (see 4.1.3). 20 ml of this inoculum was collected and centrifuged for 7 minutes at 3000 rpm and 22°C. The pellet was washed three times with PBS and resuspended in 900 μl of PBS. 100 μl of Alexa fluor 488 (1 mg/ml stock) (Life Technologies) was then added to the solution and cells were stained for 1.5 hours at 30°C with slight rotation in the dark. After staining, Candida was washed three times with PBS and resuspended in 1 ml of PBS.

Primary dendritic cells were differentiated as described in 4.1.2. Cells were then plated in 6 well plates with $4*10^5$ cells per well. After incubation at 37°C in 5% CO_2 atmosphere for one day, cells were infected with stained *C. glabrata* at a MOI of 1:2 (BMDCs:Candida). Cells were then removed at indicated time points from the wells by gently scraping with a rubber cell scraper. The cells were centrifuged for 7 minutes at 300 rcf and 4°C and washed two times with cold PBS. External signal caused by adhering Candida was quenched by adding 500 μl of Trypan Blue (Sigma) to the tubes. The samples were incubated on ice for 15 minutes followed by washing with cold PBS three times. The final sample was resuspended in 400 μl of FACS fix buffer (PBS + 1% FCS + 4% formaldehyde). FACS analysis was performed using a FACS Calibur (BD Biosciences) and the software FlowJo Version 8.8.7 (Tree Star, Inc.). Unstained and stained Candida was used as a control, as well as uninfected DCs. 2 independent technical replicates were used for the phagocytosis assay.

5.1.11 Survival assay of *C. glabrata* in DCs

Primary dendritic cells were differentiated as described in 4.1.2. Cells were then plated in 96 well plates with $3*10^5$ cells per well. After incubation at 37°C in 5% CO_2 atmosphere for one day, cells were infected with wild type *C. glabrata* and the *C. glabrata* knockouts respectively at an MOI of 1:2 (BMDCs:Candida). At indicated time points, cells were lysed by roughly scraping with a pipette tip. The sample was then diluted to a final volume of 1 ml with PBS. Uninfected control cells were simply lysed by roughly scraping the cells with a pipette tip. A 1:10.000 dilution of the Candida samples was plated on YPD plates and incubated at 30°C for two days. CFUs were determined by counting single colonies on the plate. In addition, the uninfected control was plated on YPD plates to exclude the possibility of contamination in the sample. 2 independent technical replicates were used for the survival assay.

5.2 Isolation and Preparation of RNA for Sequencing

5.2.1 Isolation of RNA

RNA was isolated using the SV Total RNA Isolation System provided by Promega according to the manufacturers protocol, with the following adaptions: Cells were directly scraped from the cell culture dishes using 175 µl of lysis buffer (see 4.1.4.). To break the Candida cell wall, the samples were disrupted in a Fast Prep-24 (MP Biomedicals) using RNAse free glass beats. Glass beats were removed from the sample by centrifugation for 10 minutes at 3000 rpm and 4°C. The supernatant was added to 350 µl of RNA Dilution Buffer and the samples were heated at 70°C for 3 minutes. The rest of the RNA Isolation was performed following Promegas protocol.

5.2.2 Quantity and quality control of the RNA samples

The concentration of the RNA was controlled on a NanoDrop 2000c (Thermo Scientific). The quality was determined using Bioanalyzer 2100 Nano series (Agilent).

5.2.3 rRNA depletion and fragmentation

Low Input RiboMinus Eukaryote System v2 kit (Life Technologies) was used to reduce the amount of rRNA in the sample. The depletion was performed according to the manufacturers protocol. The rRNA depletion was followed by fragmentation of the RNA using NEBNext Magnesium RNA Fragmentation buffer (New England BioLabs) according to manufacturers protocol. Cleanup of the fragmented RNA was performed using RNeasy MinElute Cleanup kit (Qiagen) according to manufacturers protocol.

5.2.4 Reverse transcription

First strand cDNA synthesis was performed using Super Script III Reverse Transcriptase (Invitrogen) according to the following protocol: 12 μl of fragmented RNA, 1,5 μl random primers (3 μg/μl) (Invitrogen) and 1,5 μl 10 mM dNTP mix (Fermentas) were incubated at 65°C for 5 minutes, followed by incubation on ice for 5 minutes. 4 μl of first strand buffer (Invitrogen) were then added together with 1 μl of 0,1 M DTT (Invitrogen), 1 μl of RNAse OUT Recombinant Ribonuclease Inhibitor (Invitrogen) and 1 μl of Reverse Transcriptase (200 units). The sample was then incubated at 25°C for 5 minutes followed by 50 minutes on 50°C and 15 minutes on 70°C.

Second strand cDNA synthesis was performed using 22 μl of single stranded cDNA, 1 μl random primers (3 μg/μl) (Invitrogen), 4 μl of dNTP mix (10mM of each nucleotide) (Fermentas), 40 μl of 5 x second strand buffer (Invitrogen), 5,5 μl DNA Polymerase I (10 U/μl) (Invitrogen), 1,3 μl DNA Ligase (10 U/μl)

(Invitrogen) and 1,4 μl of RNAse H (2 U/μl) (Invitrogen), filled up to a total volume of 200 μl with nuclease free H_2O. The sample was incubated on 16°C for 2 hours, then on ice. Cleanup of cDNA was performed using MinElute PCR Purification kit (Qiagen) according to manufacturers protocol. The concentration of the sample was checked by staining the cDNA with Quant-iT Picogreen, followed by subsequent measurement on a NanoDrop Fluorospectrophotometer ND-3300 (Thermo Scientific).

5.2.5 Sequencing

Next generation RNA sequencing was performed on an Illumina HiSeq 2000 (Illumina) using 50bp and single-end sequencing. True Seq sample preparation and RNA sequencing was carried out at the CSF NGS Unit (Vienna, Austria) (csf.ac.at). Sequencing was performed on one biological replicate.

5.3 Bioinformatical analysis of the sequencing results and data validation

5.3.1 Mapping and differential expression analysis of the data

Sequencing quality was checked using FastQC[125]. Adapters and reads with a per base quality phred score lower then 20 were trimmed with the tool Cutadapt[126]. All read mappings were performed using NextGenMap Version 0.4.11[127] against a concatenated version of the *M. musculus* reference from the Genome Reference Consortium GRCm38, version mm10 (ENSEMBL[128]) and the *C. glabrata* CBS138 genome version s02-m02-r14 available on the Candida Genome Database[37]. A minimum threshold of 90% identity for read alignment to the reference sequence was used. Using SAMtools[129], we discarded all

mappings with a mapping quality[130] lower than 20. We calculated the coverage using the equation:

$$coverage = \frac{number\ of\ total\ reads \times sequence\ read\ length}{transcriptome\ length}$$

Gene counts were obtained from mapped reads using the tool HTSeq[131]. Normalization and differential expression analysis were performed using the R package DESeq Version 1.16.0 [109], with genes being considered differentially expressed when showing an adjusted p-value lower than 0,1. Differential gene expression was visualized using the integrative genomics viewer (igv)[132,133]. GO term analysis of *C. glabrata* was carried out using the web - based application FungiFun Version 2.2.7 BETA[93].

5.3.2 Validation of the sequencing results using quantitative polymerase chain reaction (qPCR)

To obtain cDNA, the RNA was reverse transcribed using a Reverse Transcription System (Promega) according to manufacturers protocol, with the slight change of using 20 U AMV Reverse Transcriptase instead of the suggested 15 U.
Quantitative Polymerase Chain Reaction (qPCR) was used to validate the results obtained by the sequencing. Therefore between 2,5 and 5 *µ*g of cDNA were combined with 10 *µ*l of KAPA SYBR Green Mastermix (PeqLab) together with 0,2 *µ*l of 10 *µ*M Primer each, filled up with nuclease free water to a total volume of 19,6 *µ*l. Conditions for the amplification were at 95°C for 2 min, 95°C for 3 sec, 62°C for 25 sec, and 72°C for 30 sec for 40 cycles. Melting curve analysis was carried out till 95°C. Validation was performed using at least three independent biological replicates. qPCR was carried out on a realplex[4] Mastercycler (Eppendorf).

Primers:

Act1 **(house keeping gene)**   **forward 5'-** AATTGAGAGTCGCCCCAGAA **- 3'**

                                                  reverse 5' - TAACACCGTCACCAGAGTCC **- 3'**

CAGL0H02255g   **forward 5' -** CTGCGCCCAACTCATAGAAC **- 3'**

                                                  reverse 5' - TGGCGCATGATAGGCTCTAA **- 3'**

CAGL0G09449g   **forward 5' -** AGGCTGTGGACGGTGAAATA **- 3'**

                                                  reverse 5' - TGGAAGATGAACTGGCGGAT **- 3'**

CAGL0I06160g   **forward 5' -** TCAAGAACGTCGCCCTAACT **- 3'**

                                                  reverse 5' - AGCAGCAGAAGTAGCTTGGA **- 3'**

CAGL0E01771g   **forward 5' -** TTGGCATCGGTTTACCTGGA **- 3'**

                                                  reverse 5' - ATGGTCAACAGCCCCGAATA **- 3'**

CAGL0F07601g   **forward 5' -** GGTTCCGTTGTTGCTGACTT **- 3'**

                                                  reverse 5' - GTTGGTGGATGGTGGAGGTA **- 3'**

CAGL0G04851g   **forward 5' -** CCTGGATCAAGGTCCACACT **- 3'**

                                                  reverse 5' - CATTGGAGAGGCGTTGATGG **- 3'**

CAGL0G05896g   **forward 5' -** TGCCGCTACACTTTTGGTTT **- 3'**

                                                  reverse 5' - TGTGACTTCATTGTTCGCCA **- 3'**

CAGL0M03773g   **forward 5' -** CTCCATCCTCTGTTGCTCCA **- 3'**

                                                  reverse 5' - GTTCTTACCAGCGGCGTTAG **- 3'**

4.4. Statistical analysis

All statistical analysis were carried out using the software GraphPad Prism Version 6.0 (GraphPad Software, Inc.), unless stated otherwise. Statistical significance was determined as:

p-value > 0.05	not significant (ns)
p-value ≤ 0.05	*
p-value ≤ 0.01	**
p-value ≤ 0.001	***

6 References

1. Scully, C., el-Kabir, M. & Samaranayake, L. P. Candida and oral candidosis: a review. *Crit. Rev. Oral Biol. Med. Off. Publ. Am. Assoc. Oral Biol.* **5,** 125–157 (1994).

2. Lionakis, M. S. New insights into innate immune control of systemic candidiasis. *Med. Mycol.* **52,** 555–564 (2014).

3. Hobson, R. P. The global epidemiology of invasive Candida infections--is the tide turning? *J. Hosp. Infect.* **55,** 159–168; quiz 233 (2003).

4. Perez-Nadales, E. *et al.* Fungal model systems and the elucidation of pathogenicity determinants. *Fungal Genet. Biol. FG B* **70C,** (2014).

5. Csank, C. & Haynes, K. Candida glabrata displays pseudohyphal growth. *FEMS Microbiol. Lett.* **189,** 115–120 (2000).

6. Brand, A. Hyphal growth in human fungal pathogens and its role in virulence. *Int. J. Microbiol.* **2012,** (2012).

7. Butler, G. *et al.* Evolution of pathogenicity and sexual reproduction in eight Candida genomes. *Nature* **459,** 657–662 (2009).

8. Yang, Y.-L. *et al.* Comparison of human and soil Candida tropicalis isolates with reduced susceptibility to fluconazole. *PloS One* **7,** (2012).

9. McManus, B. A. & Coleman, D. C. Molecular epidemiology, phylogeny and evolution of Candida albicans. *Infect. Genet. Evol. J. Mol. Epidemiol. Evol. Genet. Infect. Dis.* **21,** 166–178 (2014).

10.   Giri, S. & Kindo, A. J. A review of Candida species causing blood stream infection. *Indian J. Med. Microbiol.* **30,** 270–278 (2012).

11.   Smeekens, S. P., van de Veerdonk, F. L., Kullberg, B. J. & Netea, M. G. Genetic susceptibility to Candida infections. *EMBO Mol. Med.* **5,** 805–813 (2013).

12.   Wisplinghoff, H. *et al.* Nosocomial bloodstream infections in US hospitals: analysis of 24,179 cases from a prospective nationwide surveillance study. *Clin. Infect. Dis. Off. Publ. Infect. Dis. Soc. Am.* **39,** 309–317 (2004).

13.   Cassone, A. & Cauda, R. Candida and candidiasis in HIV-infected patients: where commensalism, opportunistic behavior and frank pathogenicity lose their borders. *AIDS Lond. Engl.* **26,** 1457–1472 (2012).

14.   Plantinga, T. S. *et al.* Human genetic susceptibility to Candida infections. *Med. Mycol.* **50,** 785–794 (2012).

15.   Bourgeois, C. *et al.* Conventional dendritic cells mount a type I IFN response against Candida spp. requiring novel phagosomal TLR7-mediated IFN-beta signaling. *J. Immunol. Baltim. Md 1950* **186,** 3104–3112 (2011).

16.   Taylor, P. R. *et al.* Dectin-1 is required for beta-glucan recognition and control of fungal infection. *Nat. Immunol.* **8,** 31–38 (2007).

17.   Drewniak, A. *et al.* Invasive fungal infection and impaired neutrophil killing in human CARD9 deficiency. *Blood* **121,** 2385–2392 (2013).

18.   Wirnsberger, G. *et al.* Jagunal homolog 1 is a critical regulator of neutrophil function in fungal host defense. *Nat Genet* **advance online publication,** (2014).

19.   Tuite, A., Elias, M., Picard, S., Mullick, A. & Gros, P. Genetic control of susceptibility to Candida albicans in susceptible A/J and resistant C57BL/6J mice. *Genes Immun.* **6,** 672–682 (2005).

20.   Vázquez-González, D., Perusquía-Ortiz, A. M., Hundeiker, M. & Bonifaz, A. Opportunistic yeast infections: candidiasis, cryptococcosis, trichosporonosis and geotrichosis. *JDDG J. Dtsch. Dermatol. Ges.* **11,** 381–394 (2013).

21.   Williams, D. & Lewis, M. Pathogenesis and treatment of oral candidosis. *J. Oral Microbiol.* **3,** (2011).

22.   Zhang, J.-Y. *et al.* Vulvovaginal candidiasis: species distribution, fluconazole resistance and drug efflux pump gene overexpression. *Mycoses* (2014). doi:10.1111/myc.12204

23.   Sajith, K. G., Dutta, A. K., Sahni, R. D., Esakimuthu, S. & Chacko, A. Is empiric therapy with fluconazole appropriate for esophageal candidiasis? *Indian J. Gastroenterol. Off. J. Indian Soc. Gastroenterol.* **33,** 165–168 (2014).

24.   Nenoff, P., Paasch, U. & Handrick, W. [Infections of finger and toe nails due to fungi and bacteria]. *Hautarzt Z. Dermatol. Venerol. Verwandte Geb.* **65,** 337–348 (2014).

25.   Lionakis, M. S. & Netea, M. G. Candida and Host Determinants of Susceptibility to Invasive Candidiasis. *PLoS Pathog* **9,** e1003079 (2013).

26.   Lionakis, M. S., Lim, J. K., Lee, C.-C. R. & Murphy, P. M. Organ-Specific Innate Immune Responses in a Mouse Model of Invasive Candidiasis. *J. Innate Immun.* **3,** 180–199 (2011).

27.   Martin, G. S. Sepsis, severe sepsis and septic shock: changes in incidence, pathogens and outcomes. *Expert Rev. Anti Infect. Ther.* **10,** 701–706 (2012).

28.   Pappas, P. G. *et al.* Clinical practice guidelines for the management of candidiasis: 2009 update by the Infectious Diseases Society of America. *Clin. Infect. Dis. Off. Publ. Infect. Dis. Soc. Am.* **48,** 503–535 (2009).

29.   Bondaryk, M., Kurzatkowski, W. & Staniszewska, M. Antifungal agents commonly used in the superficial and mucosal candidiasis treatment: mode of action and resistance development. *Postepy Dermatol. Alergol.* **30,** (2013).

30.   Paul, S. & Moye-Rowley, S. Multidrug Resistance in Fungi: Regulation of Transporter-encoding Gene Expression. *Front. Physiol.* **5,** (2014).

31.   Costa, C., Dias, P. J., Sa-Correia, I. & Teixeira, M. C. MFS multidrug transporters in pathogenic fungi: do they have real clinical impact? *Front. Physiol.* **5,** (2014).

32.   Klein, C., Kuchler, K. & Valachovic, M. ABC proteins in yeast and fungal pathogens. *Essays Biochem.* **50,** 101–119 (2011).

33.   Fidel, P. L. J., Vazquez, J. A. & Sobel, J. D. Candida glabrata: review of epidemiology, pathogenesis, and clinical disease with comparison to C. albicans. *Clin. Microbiol. Rev.* **12,** (1999).

34.   Yanez-Carrillo, P., Robledo-Marquez, K. A., Ramirez-Zavaleta, C. Y., De Las Penas, A. & Castano, I. The mating type-like loci of Candida glabrata. *Rev. Iberoam. Micol.* **31,** 30–34 (2014).

35.   Lachke, S. A., Joly, S., Daniels, K. & Soll, D. R. Phenotypic switching and filamentation in Candida glabrata. *Microbiol. Read. Engl.* **148,** 2661–2674 (2002).

36.   Brieland, J. *et al.* Comparison of pathogenesis and host immune

responses to Candida glabrata and Candida albicans in systemically infected

immunocompetent mice. *Infect. Immun.* **69,** 5046–5055 (2001).

37.   Inglis, D. O. *et al.* The Candida genome database incorporates multiple

Candida species: multispecies search and analysis tools with curated gene

and protein information for Candida albicans and Candida glabrata. *Nucleic

Acids Res.* **40,** D667–D674 (2012).

38.   Roetzer, A., Gabaldon, T. & Schuller, C. From Saccharomyces cerevisiae

to Candida glabratain a few easy steps: important adaptations for an

opportunistic pathogen. *FEMS Microbiol. Lett.* **314,** (2011).

39.   Tscherner, M., Schwarzmüller, T. & Kuchler, K. Pathogenesis and

Antifungal Drug Resistance of the Human Fungal Pathogen Candida glabrata.

Pharmaceuticals **4,** 169–186 (2011).

40.   Kasper, L. *et al.* Identification of Candida glabrata genes involved in pH

modulation and modification of the phagosomal environment in macrophages.

PloS One **9,** (2014).

41.   Schwarzmüller, T. *et al.* Systematic Phenotyping of a Large-Scale Candida

glabrata Deletion Collection Reveals Novel Antifungal Tolerance Genes. *PLoS

Pathog* **10,** e1004211 (2014).

42.   Jacobsen, I. D. *et al.* Candida glabrata Persistence in Mice Does Not

Depend on Host Immunosuppression and Is Unaffected by Fungal Amino Acid

Auxotrophy. *Infect. Immun.* **78,** 1066–1077 (2010).

43.   Moran, C., Grussemeyer, C. A., Spalding, J. R., Benjamin, D. K. J. &

Reed, S. D. Comparison of costs, length of stay, and mortality associated with

Candida glabrata and Candida albicans bloodstream infections. *Am. J. Infect. Control* **38,** (2010).

44.   Rodrigues, C. F., Silva, S. & Henriques, M. Candida glabrata: a review of its features and resistance. *Eur. J. Clin. Microbiol. Infect. Dis. Off. Publ. Eur. Soc. Clin. Microbiol.* **33,** 673–688 (2014).

45.   Douglas, L. J. Candida biofilms and their role in infection. *Trends Microbiol.* **11,** 30–36 (2003).

46.   Kaur, R., Ma, B. & Cormack, B. P. A family of glycosylphosphatidylinositol-linked aspartyl proteases is required for virulence of Candida glabrata. *Proc. Natl. Acad. Sci.* **104,** 7628–7633 (2007).

47.   Brunke, S. & Hube, B. Two unlike cousins: Candida albicans and C. glabrata infection strategies. *Cell. Microbiol.* **15,** 701–708 (2013).

48.   Roetzer, A., Gratz, N., Kovarik, P. & Schüller, C. Autophagy supports Candida glabrata survival during phagocytosis. *Cell. Microbiol.* **12,** 199–216 (2010).

49.   Abul K. Abbas, et al. *Cellular and Molecular Immunology*. (Saunders).

50.   Liu, K. & Nussenzweig, M. C. Origin and development of dendritic cells. *Immunol. Rev.* **234,** 45–54 (2010).

51.   Ni, K. & O'Neill, H. C. The role of dendritic cells in T cell activation. *Immunol. Cell Biol.* **75,** 223–230 (1997).

52.   SNELL, G. D. & HIGGINS, G. F. Alleles at the histocompatibility-2 locus in the mouse as determined by tumor transplantation. *Genetics* **36,** 306–310 (1951).

53.   Neefjes, J., Jongsma, M. L. M., Paul, P. & Bakke, O. Towards a systems understanding of MHC class I and MHC class II antigen presentation. *Nat Rev Immunol* **11,** 823–836 (2011).

54.   Reis e Sousa, C. Dendritic cells in a mature age. *Nat Rev Immunol* **6,** 476–483 (2006).

55.   Schuler, G. & Steinman, R. M. Murine epidermal Langerhans cells mature into potent immunostimulatory dendritic cells in vitro. *J. Exp. Med.* **161,** 526–546 (1985).

56.   Satpathy, A. T., Wu, X., Albring, J. C. & Murphy, K. M. Re(de)fining the dendritic cell lineage. *Nat Immunol* **13,** 1145–1154 (2012).

57.   Steinman, R. M. & Inaba, K. Myeloid dendritic cells. *J. Leukoc. Biol.* **66,** 205–208 (1999).

58.   Ziegler-Heitbrock, L. A., Petronela Crowe, Suzanne Dalod, Marc Grau, Veronika Hart, Derek N. Leenen, Pieter J. M. Liu, Yong-Jun MacPherson, Gordon Randolph, Gwendalyn J. Scherberich, Juergen Schmitz, Juergen Shortman, Ken Sozzani, Silvano Strobl, Herbert Zembala, Marek Austyn, Jonathan M. Lutz, Manfred B. Nomenclature of monocytes and dendritic cells in blood. *Blood* **116,** e74–e80 (2010).

59.   Kim, S. J. & Diamond, B. Generation and maturation of bone marrow-derived DCs under serum-free conditions. *J. Immunol. Methods* **323,** 101–108 (2007).

60.   Vremec, D. *et al.* Maintaining dendritic cell viability in culture. *Mol. Immunol.* (2014). doi:10.1016/j.molimm.2014.07.011

61.   Kinchen, J. M. & Ravichandran, K. S. Phagosome maturation: going through the acid test. *Nat Rev Mol Cell Biol* **9,** 781–795 (2008).

62.   Haas, A. The Phagosome: Compartment with a License to Kill. *Traffic* **8,** 311–330 (2007).

63.   Seider, K. *et al.* The facultative intracellular pathogen Candida glabrata subverts macrophage cytokine production and phagolysosome maturation. *J. Immunol. Baltim. Md 1950* **187,** 3072–3086 (2011).

64.   Seider, K. *et al.* Immune evasion, stress resistance, and efficient nutrient acquisition are crucial for intracellular survival of Candida glabrata within macrophages. *Eukaryot. Cell* **13,** 170–183 (2014).

65.   Garcia-Rodas, R., Gonzalez-Camacho, F., Rodriguez-Tudela, J. L., Cuenca-Estrella, M. & Zaragoza, O. The interaction between Candida krusei and murine macrophages results in multiple outcomes, including intracellular survival and escape from killing. *Infect. Immun.* **79,** 2136–2144 (2011).

66.   Isaacs, A. & Lindenmann, J. Virus Interference. I. The Interferon. *Proc. R. Soc. Lond. Ser. B - Biol. Sci.* **147,** 258–267 (1957).

67.   Stanton, G. J., Weigent, D. A., Fleischmann, W. R. J., Dianzani, F. & Baron, S. Interferon review. *Invest. Radiol.* **22,** 259–273 (1987).

68.   Bogdan, C., Mattner, J. & Schleicher, U. The role of type I interferons in non-viral infections. *Immunol. Rev.* **202,** (2004).

69.   Platanias, L. C. Mechanisms of type-I- and type-II-interferon-mediated signalling. *Nat. Rev. Immunol.* **5,** 375–386 (2005).

70.   Manry, J. *et al.* Evolutionary genetic dissection of human interferons. *J. Exp. Med.* **208,** 2747–2759 (2011).

71.   Majer, O. *et al.* Type I interferons promote fatal immunopathology by regulating inflammatory monocytes and neutrophils during Candida infections. *PLoS Pathog.* **8,** (2012).

72.   Ivashkiv, L. B. & Donlin, L. T. Regulation of type I interferon responses. *Nat Rev Immunol* **14,** 36–49 (2014).

73.   González-Navajas, J. M., Lee, J., David, M. & Raz, E. Immunomodulatory functions of type I interferons. *Nat Rev Immunol* **12,** 125–135 (2012).

74.   Horvath, C. M. & Darnell, J. E. The antiviral state induced by alpha interferon and gamma interferon requires transcriptionally active Stat1 protein. *J. Virol.* **70,** 647–650 (1996).

75.   Schroder, K., Hertzog, P. J., Ravasi, T. & Hume, D. A. Interferon-gamma: an overview of signals, mechanisms and functions. *J. Leukoc. Biol.* **75,** 163–189 (2004).

76.   Biondo, C. *et al.* Recognition of yeast nucleic acids triggers a host-protective type I interferon response. *Eur. J. Immunol.* **41,** 1969–1979 (2011).

77.   Mortazavi, A., Williams, B. A., McCue, K., Schaeffer, L. & Wold, B. Mapping and quantifying mammalian transcriptomes by RNA-Seq. *Nat Meth* **5,** 621–628 (2008).

78.   Chu, Y. & Corey, D. R. RNA sequencing: platform selection, experimental design, and data interpretation. *Nucleic Acid Ther.* **22,** 271–274 (2012).

79.   Zhao, W. *et al.* Comparison of RNA-Seq by poly (A) capture, ribosomal RNA depletion, and DNA microarray for expression profiling. *BMC Genomics* **15,** (2014).

80.   Wang, Z., Gerstein, M. & Snyder, M. RNA-Seq: a revolutionary tool for transcriptomics. *Nat Rev Genet* **10,** 57–63 (2009).

81.   Grabherr, M. G. *et al.* Full-length transcriptome assembly from RNA-Seq data without a reference genome. *Nat Biotech* **29,** 644–652 (2011).

82.   Lowe, R. G. T. *et al.* Genomes and Transcriptomes of Partners in Plant-Fungal- Interactions between Canola (Brassica napus) and Two Leptosphaeria Species. *PloS One* **9,** (2014).

83.   Longo, A. V., Burrowes, P. A. & Zamudio, K. R. Genomic studies of disease-outcome in host-pathogen dynamics. *Integr. Comp. Biol.* **54,** 427–438 (2014).

84.   Camilios-Neto, D. *et al.* Dual RNA-seq transcriptional analysis of wheat roots colonized by Azospirillum brasilense reveals up-regulation of nutrient acquisition and cell cycle genes. *BMC Genomics* **15,** (2014).

85.   Choi, Y.-J., Aliota, M. T., Mayhew, G. F., Erickson, S. M. & Christensen, B. M. Dual RNA-seq of parasite and host reveals gene expression dynamics during filarial worm-mosquito interactions. *PLoS Negl. Trop. Dis.* **8,** (2014).

86.   Tierney, L. *et al.* An Interspecies Regulatory Network Inferred from Simultaneous RNA-seq of Candida albicans Invading Innate Immune Cells. *Front. Microbiol.* **3,** (2012).

87.   Tierney, L., Kuchler, K., Rizzetto, L. & Cavalieri, D. Systems biology of host-fungus interactions: turning complexity into simplicity. *Curr. Opin. Microbiol.* **15,** 440–446 (2012).

88.   Pepke, S., Wold, B. & Mortazavi, A. Computation for ChIP-seq and RNA-seq studies. *Nat Meth* **6,** S22–S32 (2009).

89.   Koboldt, D. C., Steinberg, K. M., Larson, D. E., Wilson, R. K. & Mardis, E.
R. The Next-Generation Sequencing Revolution and Its Impact on Genomics.
Cell **155,** 27–38

90.   Ning, S., Pagano, J. S. & Barber, G. N. IRF7: activation, regulation,
modification and function. *Genes Immun.* **12,** (2011).

91.   Eder, C. Mechanisms of interleukin-1beta release. *Immunobiology* **214,**
543–553 (2009).

92.   Ashburner, M. *et al.* Gene ontology: tool for the unification of biology. The
Gene Ontology Consortium. *Nat. Genet.* **25,** 25–29 (2000).

93.   Priebe, S., Linde, J., Albrecht, D., Guthke, R. & Brakhage, A. A. FungiFun:
a web-based application for functional categorization of fungal genes and
proteins. *Fungal Genet. Biol. FG B* **48,** 353–358 (2011).

94.   Subramanian, A. *et al.* Gene set enrichment analysis: A knowledge-based
approach for interpreting genome-wide expression profiles. *Proc. Natl. Acad.
Sci. U. S. A.* **102,** 15545–15550 (2005).

95.   Manning, B. D., Padmanabha, R. & Snyder, M. The Rho-GEF Rom2p
localizes to sites of polarized cell growth and participates in cytoskeletal
functions in Saccharomyces cerevisiae. *Mol. Biol. Cell* **8,** 1829–1844 (1997).

96.   Mehdi, K., Thierie, J. & Penninckx, M. J. gamma-Glutamyl transpeptidase
in the yeast Saccharomyces cerevisiae and its role in the vacuolar transport
and metabolism of glutathione. *Biochem. J.* **359,** 631–637 (2001).

97.   Cabib, E. *et al.* Assembly of the yeast cell wall. Crh1p and Crh2p act as
transglycosylases in vivo and in vitro. *J. Biol. Chem.* **283,** 29859–29872
(2008).

98.   Wadskog, I. *et al.* The yeast tumor suppressor homologue Sro7p is

required for targeting of the sodium pumping ATPase to the cell surface. *Mol.*

Biol. Cell **17,** (2006).

99.   Jochems, C. E. A., van der Valk, J. B. F., Stafleu, F. R. & Baumans, V.

The use of fetal bovine serum: ethical or scientific problem? *Altern. Lab. Anim.*

ATLA **30,** 219–227 (2002).

100.   Heilmann, C. J. *et al.* Hyphal induction in the human fungal pathogen

Candida albicans reveals a characteristic wall protein profile. *Microbiology* **157,**

2297–2307 (2011).

101.   Sudbery, P. E. Growth of Candida albicans hyphae. *Nat Rev Micro* **9,** 737–

748 (2011).

102.   Nagi, M. *et al.* Serum cholesterol promotes the growth of Candida glabrata

in the presence of fluconazole. *J. Infect. Chemother. Off. J. Jpn. Soc.*

Chemother. **19,** 138–143 (2013).

103.   Nagi, M. *et al.* The Candida glabrata sterol scavenging mechanism,

mediated by the ATP-binding cassette transporter Aus1p, is regulated by iron

limitation. *Mol. Microbiol.* **88,** 371–381 (2013).

104.   Sultan, M. *et al.* Influence of RNA extraction methods and library selection

schemes on RNA-seq data. *BMC Genomics* **15,** (2014).

105.   Ajay, S. S., Parker, S. C. J., Ozel Abaan, H., Fuentes Fajardo, K. V. &

Margulies, E. H. Accurate and comprehensive sequencing of personal

genomes. *Genome Res.* **21,** 1498–1505 (2011).

106.   Metpally, R. P. R. *et al.* Comparison of analysis tools for miRNA high

throughput sequencing using nerve crush as a model. *Front. Genet.* **4,** (2013).

107.   Bizon, C. *et al.* Variant calling in low-coverage whole genome sequencing of a Native American population sample. *BMC Genomics* **15,** 85 (2014).

108.   Le, S. Q. & Durbin, R. SNP detection and genotyping from low-coverage sequencing data on multiple diploid samples. *Genome Res.* **21,** 952–960 (2011).

109.   Anders, S. & Huber, W. Differential expression analysis for sequence count data. *Genome Biol.* **11,** (2010).

110.   Auer, P. L. & Doerge, R. W. Statistical Design and Analysis of RNA Sequencing Data. *Genetics* **185,** 405–416 (2010).

111.   Marioni, J. C., Mason, C. E., Mane, S. M., Stephens, M. & Gilad, Y. RNA-seq: An assessment of technical reproducibility and comparison with gene expression arrays. *Genome Res.* **18,** 1509–1517 (2008).

112.   Sims, D., Sudbery, I., Ilott, N. E., Heger, A. & Ponting, C. P. Sequencing depth and coverage: key considerations in genomic analyses. *Nat Rev Genet* **15,** 121–132 (2014).

113.   Scuderi, S., La Cognata, V., Drago, F., Cavallaro, S. & D'Agata, V. Alternative Splicing Generates Different Parkin Protein Isoforms: Evidences in Human, Rat, and Mouse Brain. *BioMed Res. Int.* **2014,** (2014).

114.   De Groot, P. W. J. *et al.* The Cell Wall of the Human Pathogen Candida glabrata: Differential Incorporation of Novel Adhesin-Like Wall Proteins. *Eukaryot. Cell* **7,** 1951–1964 (2008).

115.   De Groot, P. W. J., Ram, A. F. & Klis, F. M. Features and functions of covalently linked proteins in fungal cell walls. *Fungal Genet. Biol. FG B* **42,** 657–675 (2005).

116. Weig, M. *et al.* Systematic identification in silico of covalently bound cell wall proteins and analysis of protein–polysaccharide linkages of the human pathogen Candida glabrata. *Microbiology* **150,** 3129–3144 (2004).

117. Cabezon, V., Llama-Palacios, A., Nombela, C., Monteoliva, L. & Gil, C. Analysis of Candida albicans plasma membrane proteome. *Proteomics* **9,** 4770–4786 (2009).

118. Halliwell, S. C., Smith, M. C. A., Muston, P., Holland, S. L. & Avery, S. V. Heterogeneous Expression of the Virulence-Related Adhesin Epa1 between Individual Cells and Strains of the Pathogen Candida glabrata. *Eukaryot. Cell* **11,** 141–150 (2012).

119. Kempf, M. *et al.* Disruption of the GPI protein-encoding gene IFF4 of Candida albicans results in decreased adherence and virulence. *Mycopathologia* **168,** 73–77 (2009).

120. Vale-Silva, L., Ischer, F., Leibundgut-Landmann, S. & Sanglard, D. Gain-of-Function Mutations in PDR1, a Regulator of Antifungal Drug Resistance in Candida glabrata, Control Adherence to Host Cells. *Infect. Immun.* **81,** 1709–1720 (2013).

121. Fu, Y., Luo, G., Spellberg, B. J., Edwards, J. E. & Ibrahim, A. S. Gene Overexpression/Suppression Analysis of Candidate Virulence Factors of Candida albicans. *Eukaryot. Cell* **7,** 483–492 (2008).

122. Rai, M. N., Sharma, V., Balusu, S. & Kaur, R. An essential role for phosphatidylinositol 3-kinase in the inhibition of phagosomal maturation, intracellular survival and virulence in Candida glabrata. *Cell. Microbiol.* (2014). doi:10.1111/cmi.12364

123.	West, L. *et al.* Differential virulence of Candida glabrata glycosylation

	mutants. *J. Biol. Chem.* **288,** 22006–22018 (2013).

124.	Turner, S. A. & Butler, G. The Candida Pathogenic Species Complex. *Cold*

	Spring Harb. Perspect. Med. **4,** (2014).

125.	Andrews, S. FastQC A Quality Control tool for High Throughput Sequence

	Data. *http://www.bioinformatics.babraham.ac.uk/projects/fastqc/* at

	<http://www.bioinformatics.babraham.ac.uk/projects/fastqc/>

126.	Martin, M. Cutadapt removes adapter sequences from high-throughput

	sequencing reads. *EMBnet.journal* **17,** (2011).

127.	Sedlazeck, F. J., Rescheneder, P. & von Haeseler, A. NextGenMap: fast

	and accurate read mapping in highly polymorphic genomes. *Bioinforma. Oxf.*

	Engl. **29,** 2790–2791 (2013).

128.	Flicek, P. *et al.* Ensembl 2014. *Nucleic Acids Res.* **42,** D749–D755 (2014).

129.	Li, H. *et al.* The Sequence Alignment/Map format and SAMtools.

	Bioinformatics **25,** 2078–2079 (2009).

130.	Li, H., Ruan, J. & Durbin, R. Mapping short DNA sequencing reads and

	calling variants using mapping quality scores. *Genome Res.* **18,** 1851–1858

	(2008).

131.	Anders, S. P., Paul Theodor Huber, Wolfgang. HTSeq - A Python

	framework to work with high-throughput sequencing data. *bioRxiv* (2014).

	doi:10.1101/002824

132.	Robinson, J. T. *et al.* Integrative genomics viewer. *Nat Biotech* **29,** 24–26

	(2011).

133. Thorvaldsdóttir, H., Robinson, J. T. & Mesirov, J. P. Integrative Genomics

   Viewer (IGV): high-performance genomics data visualization and exploration.

   Brief. Bioinform. **14,** 178–192 (2013).

7 Appendix

7.1 Zusammenfassung

Candida glabrata (*C. glabrata*) ist einer der am häufigsten vorkommenden Pilz - Pathogene im Menschen. Er verursacht keine Infektionen in gesunden Wirten, kann allerdings ernstzunehmende Krankheiten in immunsupprimierten Individuen auslösen. Dort befällt er vor allem Schleimhäute, kann sich aber auch systemisch durch den Blutkreislauf verbreiten. Aufgrund des hohen Anstiegs an immunsupprimierten Patienten in den letzten Jahren wurden Infektionen der Gattung Candida zu einem bedeutendem Gesundheitsproblem, wobei *C. glabrata* für etwa 15% der systemischen Infektionen weltweit verantwortlich ist. Dendritische Zellen spielen eine tragende Rolle während einer Infektion mit *C. glabrata*, da sie im Körper die Aufgabe Antigen - präsentierender Zellen übernehmen. Es ist bekannt, dass Typ I Interferone (type I IFNs) maßgeblich an der Entstehung von Entzündungen beteiligt sind, und diese Signalstoffe daher eine wichtige Rolle während einer Infektion spielen. Kürzlich wurde gezeigt, dass Type I IFNs auch eines der wichtigsten Signalmoleküle während der Infektion mit Candida sind. Während des Experiments wurden Dendritische Zellen aus Knochenmarksstammzellen der Maus differenziert, um ihre Abwehrkraft gegen eindringende Pathogene *in vitro* zu beobachten. Weiters wurden diese Zellen mit *C. glabrata* infiziert, um eine zeitabhängige Isolierung von Maus- und Candida RNA zu durchzuführen. Um den Zusammenhang zwischen type I IFNs und Candida - Infektionen besser zu verstehen, wurde das Experiment nicht nur mit Wild Typ Mäusen, sondern auch mit Mäusen durchgeführt, die einen Defekt in der Signalweiterleitung durch type I IFNs haben (*Ifnar1$^{-/-}$*). Diesen Mäusen fehlt eine funktionelle Untereinheit des type I IFN Rezeptors. Es ist ihnen daher nicht möglich, type I IFNs abhängige Signale aus der Umwelt aufzunehmen. Um unsere Fragestellung zu erläutern, entschieden wir uns für eine Methode namens „parallel dual - species RNA Sequenzierung" (RNA Seq). Diese High Throughput Methode liefert innerhalb kurzer Zeit eine große Menge an Informationen, und

ermöglicht es, nicht nur Daten eines Organismus zu erfassen, sondern mehrerer Organismen gleichzeitig. Nach der Sequenzierung wurden die Daten bioinformatisch analysiert. Diese Verfahrensweise ermöglichte es uns, Gene in beiden Organismen zu identifizieren, die zeitabhängig differenziell exprimiert wurden. Wir erstellten eine Liste an gene ontology (GO) terms um die Bedeutung bestimmter Gen - Gruppen und deren komplexes Zusammenwirken aufzuzeigen. Zusätzlich konnten wir 3 Gene in *C. glabrata* identifizieren, die während einer Infektion wichtig erscheinen, da wir zeigen konnten, dass der Verlust dieser Gene eine geringere Überlebensrate des Fungus während einer Infektion zur Folge hatte. Unseres Wissens nach, wurden diese Gene bisher nicht mit Infektionen assoziiert.

7.2 Short Curriculum Vitae

Education

05/2013 - 10/2014
Masterthesis in the Laboratory of Prof. Dr. Karl Kuchler, Max F. Perutz Laboratories, Vienna, Austria

09/2012 - 01/2012
Semester Abroad at the University of Leicester, England

03/2012 - 10/2014
Master of Microbiology and Immunobiology at the University of Vienna, Austria

07/2007 - 12/2011
Bachelor of Biology at the University of Vienna, Austria, with Focus on Microbiology and Genetics

05/2007
General Qualification for University Entrance at the Bundesgymnasium/ Bundesrealgymnasium Sankt Pölten, Austria

Work experience

2013/2014
Lecturing Tutor in Biochemistry, University of Vienna, Austria

07/2010
Laboratory Assistant at BAXTER Vienna, Austria, with Focus on Quality Control

07/2008/2009
Medical Assistant in the Office of Dr. Michael Stolz MAS, Doctor for General Medicine in Rabenstein/ Pielach, Austria

Congresses

06/2014
10th YSA-PhD-Symposium, Young Scientist Association
Poster Presentation: "Deciphering the Immune Response in Murine Bone Marrow - Derived Dendritic Cells to the Opportunistic Fungal Pathogen *Candida glabrata* Using an RNA Sequencing Approach"

09/2014

6th OEGMBT Annual Meeting, Österreichische Gesellschaft für Molekulare
Biowissenschaften und Biotechnologie
Short Talk and Poster Presentation: "Deciphering the Immune Response in Murine Bone
Marrow - Derived Dendritic Cells to the Opportunistic Fungal Pathogen *Candida glabrata*
Using an RNA Sequencing Approach"

Advanced trainings

02/2014

Introduction to Laboratory Animal Science, certified by the GV-SOLAS as FELASA
Category B
Department of Biomedical Sciences, University of Veterinary Medicine, Vienna, Austria

Personal skills/Competences

Mother tongue	German
Other languages	English (Proficient user)
	Cambridge First Certificate
	French (Independent user)
	Spanish (Independent user)

7.3 Abbreviations

Actin 1 - Act1
AIDS - Acquired Immunodeficiency Syndrome
AP-1 - Activator Protein 1
BMDCs - Bone Marrow - Derived Dendritic Cells
C. albicans - *Candida albicans*
C. glabrata - *Candida glabrata*
cDNA - complementary Deoxyribonucleic Acid
CFU - Colony Forming Unit
DC - Dendritic Cell
DMEM - Dulbecco's Modified Eagle Medium
EPA - Epithelial Adhesin
FCS - Fetal Calf Serum
GO - Gene Ontology
HLA - Human Leukocyte Antigen
Ifnar - Interferon - α/β receptor gene
igv - integrative genomics viewer
IL-1β - Interleukin - 1 beta
IRF - Interferon Regulatory Factor
ISGF3 - Interferon - Stimulated Gamma Factor 3
Jagn1 - Jagunal homolog 1
KO - Knockout
mDCs - myeloid Dendritic Cells
MHC - Major Histocompatibility Complex
NAD+ - Nicotinamide Adenine Dinucleotide
NF-κB - Nuclear Factor Kappa - Light - Chain - Enhancer of Activated B Cells
ORF - Open Reading Frame
qPCR - quantitative real - time Polymerase Chain Reaction
RIN - RNA Integrity Number
RNA - Ribonucleic Acid
RNA Seq - RNA sequencing
RNS - Reactive Nitrogen Species
ROS - Reactive Oxygen Species
STAT - Signal Transducers and Activators of Transcription
TF - Transcription Factor
Type I IFNs - Type I Interferons
Type II IFNs - Type II Interferons
Type III IFNs - Type III Interferon
WT - Wild type
YPD - Yeast Extract Peptone Dextrose

7.4 Acknowledgements

First of all I want to thank my Professor Dr. Karl Kuchler for giving me the opportunity to make my master thesis in his lab and for giving me the chance to work on such a complex topic like RNA sequencing. I also want to thank you for the courses and congresses I could visit due to your help. I learned many new methods and techniques during my time here, and I can honestly say that my time in your lab prepared me well for my scientific future.

Also, I want to thank my supervisor Florian Zwolanek, who taught me everything I needed to know about cell culture, laboratory animal science and many other things. Thank you for your patience when showing me new things, always taking time to explain stuff to me and, last but not least, correcting my master thesis.

Next, I want to thank my friend and colleague Daniel Paiva Agustinho, who spent hours with me in front of the computer helping me analyzing sequencing data, explaining statistics to me and teaching me bioinformatics. Without you, I still wouldn't know how R works…

Of course, I want to thank the whole Kuchler Group. Working with you was a great experience, and I thank you for all the support and tips that you gave me whenever I needed them. Thank you also for all the fun times we had, like rafting, paint ball and the many happy hours!

Additionally, I want to thank my family: My parents Helga, Michael and Eva and my brother Lukas for supporting me throughout my studies and helping me whenever they could. Also, I want to thank my friends, especially Sabrina for the many talks we had about work - related and non - work - related stuff. Without you, the last 15 years would have been only half the fun.